THE FINE STRUCTURE OF ACOUSTIC GANGLIA IN THE RAT

JACK ROSENBLUTH, M.D.

From the Laboratory of Neuroanatomical Sciences, National Institute of Neurological Diseases and Blindness, National Institutes of Health, Bethesda, Maryland. Dr. Rosenbluth's present address is Department of Anatomy, University of California School of Medicine, San Francisco

ABSTRACT

Nerve cell bodies in the spiral and vestibular ganglia of the adult rat are surrounded by thin (about ten lamellae) myelin sheaths which differ in several respects from typical axonal myelin. In some instances lamellae surrounding perikarya appear as typical major dense lines, and in others as thin Schwann cell sheets in which cytoplasm persists. Discontinuities and irregularities appear in the structure of perikaryal myelin. Lamellae may terminate anywhere within the sheaths; they may bifurcate; they may reverse their direction; or they may merge with each other. The number of lamellae varies from one part of a sheath to another. In addition, the myelin of a single perikaryal sheath may receive contributions from more than one Schwann cell, which overlap and interleave with each other. The ganglion cells are of two types: those which are densely packed with the usual cytoplasmic organelles but have few neurofilaments (granular neurons), and those which exhibit large areas containing few organelles but have a high concentration of neurofilaments (filamented neurons). The latter cell type is ensheathed by myelin which is generally more compact that that surrounding the former. The formation and the physiologic significance of perikaryal myelin are discussed.

INTRODUCTION

In a previous study (38) carried out on the eighth cranial nerve ganglion of the adult goldfish it was found that each bipolar ganglion cell body is contained within one internodal segment of an acoustic nerve fiber, and that the enveloping sheath of this particular segment has certain distinctive characteristics. The most important of these are: (*a*) The sheath contains from two to ninety lamellae of myelin, which is of two types—compact, consisting of alternating major dense lines and intermediate lines, and loose, consisting of multiple thin sheets of Schwann cell cytoplasm. (*b*) The number of myelin lamellae covering the perikaryal segment is generally several times smaller than that ensheathing the remaining portions of the same fiber. (*c*) The perikaryal internode may have more than one Schwann cell spatially related to it.

One of the questions raised by these observations is whether perikaryal myelin develops in the same manner as has been proposed for peripheral axonal myelin (11, 31, 32), *i.e.* by the spiral wrapping of a Schwann cell around each internodal segment, or whether a more complex mode of development occurs here, perhaps involving the interaction of several Schwann cells. Because of the large perimeter of goldfish acoustic ganglion cells and the large number of lamellae in their sheaths, it was not possible to trace the continuity of the lamellae completely in order to determine what structural patterns occur in this type of myelin. However, a detailed investigation of this

kind is feasible in mammals, for in this class of vertebrates the myelin surrounding acoustic ganglion cell bodies is thin (24), and presumably contains relatively few lamellae, whose course can be followed more readily. As in the goldfish, several Schwann cell nuclei are in some cases associated with a single perikaryal sheath (24). Furthermore, recent electron microscopic studies (25) indicate that node-like discontinuities may occur in mammalian perikaryal myelin, also suggesting that their structural pattern is more complex than a simple spiral.

The principal purpose of the present investigation was to ascertain what the ultrastructural organization of adult perikaryal myelin is in the rat, and whether or not this pattern is consistent with a simple helical genesis. In addition, a comparison of these ganglia in the rat and in the goldfish would indicate which fine structural features of acoustic ganglia are peculiar to the species and which probably occur more generally. The occurrence of two types of neuronal cytoplasm and the existence of loose myelin in adult animals were points of particular interest.

MATERIALS AND METHODS

Specimens were obtained from both the spiral and vestibular ganglia of mature Osborn-Mendel albino rats weighing approximately 150 gm. After fasting overnight, the rats were anesthetized with chloral hydrate (0.4 mg per gm) (2). Fixation was carried out by Dr. S. L. Palay, using the method of perfusion through the left ventricle (27) with 1 per cent osmium tetroxide in acetate-veronal buffer (pH 7.4 to 7.5) to which 5.4 mg per ml of calcium chloride was added. Tissues were dehydrated in methanol and embedded in Epon 812 (22). Sectioning was performed on a Porter-Blum microtome using glass or Vycor (10) knives. The sections were mounted on grids with or without a carbon substrate and stained with saturated aqueous uranyl acetate (51). Electron micrographs were taken with an RCA EMU-3E electron microscope at magnifications of 1500 to 25,000.

OBSERVATIONS

The spiral and vestibular ganglia of the rat display approximately the same cytologic features and consequently will be described together here. Preliminary examination of these ganglia by

FIGURE 1

Granular cochlear ganglion cell, 20 × 30 μ, showing both poles. The cytoplasm contains many mitochondria, which are arrayed around the nucleus, and discrete Nissl bodies peripherally. The sheath around the perikaryon and the initial portions of its neurites is dark gray, in contrast with the black myelin sheath surrounding the continuation of the upper axon. Several large mitochondria (arrows) are present in the perikaryal sheath. The first node of Ranvier (*n*) is about 12 μ from the perikaryon. × 2500.

FIGURE 2

Filamented cochlear ganglion cell, 30 × 40 μ. The cytoplasm of this neuron appears less compact than that in Fig. 1. Mitochondria and Nissl substance are more dispersed. The sheath around this cell consists of a thin but very dense inner component surrounded by a thicker layer of Schwann cell cytoplasm. A large mitochondrion occurs in the initial segment of the axon at the very top of the figure. × 2500.

FIGURE 3

Adjacent cochlear ganglion cells. The cell on the left is of the type shown in Fig. 1. It contains an abundance of granular endoplasmic reticulum but few neurofilaments or tubules. At the arrow the sheath around this neuron consists of two loose lamellae externally, five semicompact lamellae, and three loose lamellae adjacent to the neuronal surface. The neuron on the right is of the type shown in Fig. 2. It displays few ribonucleoprotein particles but many neurofilaments and tubules (in cross-section). At the arrow its sheath consists of two loose lamellae externally, one semicompact lamella, four compact lamellae, and two more loose lamellae adjacent to the neuron. *d*, dense inclusion body; *v*, multivesicular body. × 23,000.

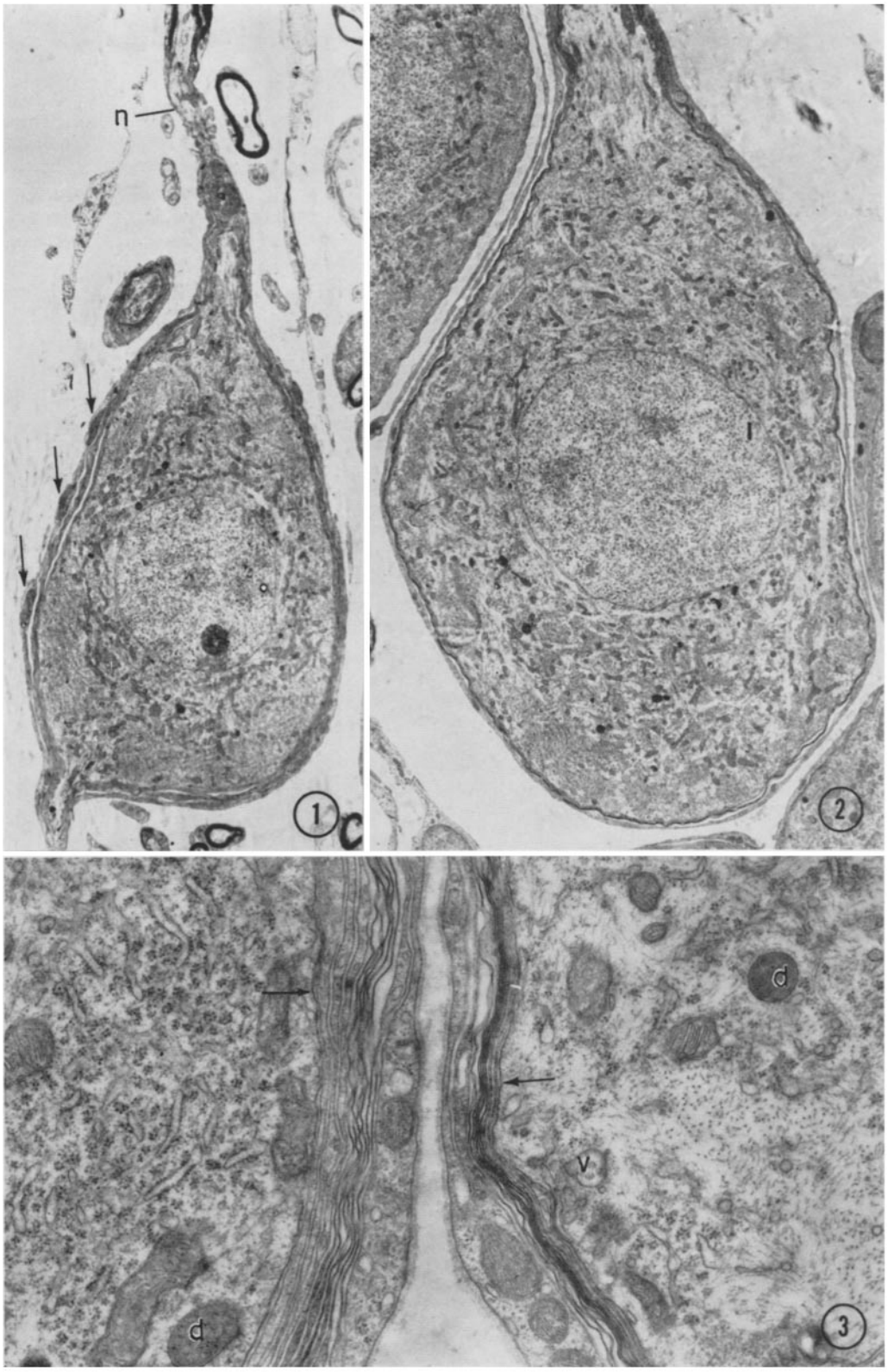
n
1
2
l
d
v
d
3

means of phase contrast microscopy of 1 to 2 μ sections shows that they bear a strong resemblance to dorsal root ganglia of the same species except for the presence of thin myelin around the cell bodies. The perikarya are spheroidal and closely packed together as noted previously (55). No greatly elongated cell bodies invested with thick compact myelin occur here as they do in the eighth nerve ganglion of the goldfish (38). Although earlier light microscopic studies indicate that these neurons are bipolar, this is not immediately apparent, probably, as Kolmer pointed out (21), because the two poles are not directly opposite to each other, so that the probability of a section's passing through both axons is greatly reduced.

Neurons

Figs. 1 and 2 are low power electron micrographs showing typical examples of the two types of neurons found in these ganglia. The first, or granular, type is illustrated in Fig. 1. Its cytoplasm appears relatively dense and contains discrete Nissl bodies peripherally plus a ring of small mitochondria around the nucleus. The nucleus contains a single nucleolus and exhibits several infoldings of its envelope. The origins of both neurites happen to be present in this section. The upper one is probably continuous with the typically myelinated axon at the top of the figure. The sheath around this cell is only slightly denser than the neuronal cytoplasm itself, and it contains several large mitochondria (arrows). Fig. 2 illustrates the second, or filamented, type. The cell shown here is considerably larger than that in Fig. 1. Its Nissl bodies are less discrete; its mitochondria are sparser and more dispersed; and there are clear areas in its cytoplasm comparable to that at the axon hillock region of the cell. Note that in the initial segment of the axon there is a mitochondrion which is considerably larger than those in the perikaryon. The sheath around this cell is distinctly denser than that in Fig. 1, although very

FIGURE 4

Compact perikaryal sheath showing terminations of several lamellae. The loose lamella adjacent to the neuron at the left of the figure is continuous with a major dense line which becomes the fourth lamella from the neuronal surface near the right side of the figure. Four lamellae terminate as blind loops of cytoplasm (arrows), three against the neuronal plasmalemma and the remaining one between the first and third lamellae on the left. × 59,000.

FIGURE 5

Detail of Fig. 6 showing part of a subsurface cistern. Its superficial surface lies ~90 A from the neuronal plasmalemma (*p*). Its deep surface is studded with ribonucleoprotein particles. The lumen of the cistern is ~200 A wide except in its bulbous ending at the left of the figure. × 70,000.

FIGURE 6

Cochlear ganglion cell showing three subsurface cisterns (arrows). That on the extreme left is 2 μ long. That in the middle has a second cistern associated with its deep surface. The neuronal cytoplasm contains a dense inclusion body (*d*), two multivesicular bodies (*v*), and two large heterogeneous bodies (*h*). The sheath over this neuron displays three blind endings. The outermost lamella at the right side of the sheath makes a U-turn around two of them and continues back toward the right as the fourth lamella from the outside. It becomes a major dense line at the extreme right. × 22,000.

FIGURE 7

Cochlear ganglion cell containing two flattened cisterns of endoplasmic reticulum, which resemble the subsurface cistern in Fig. 5. Their lumina narrow to ~90 A except in their bulbous endings. A third cistern of the usual dimensions underlies these two. No ribonucleoprotein granules lie between them. × 62,000.

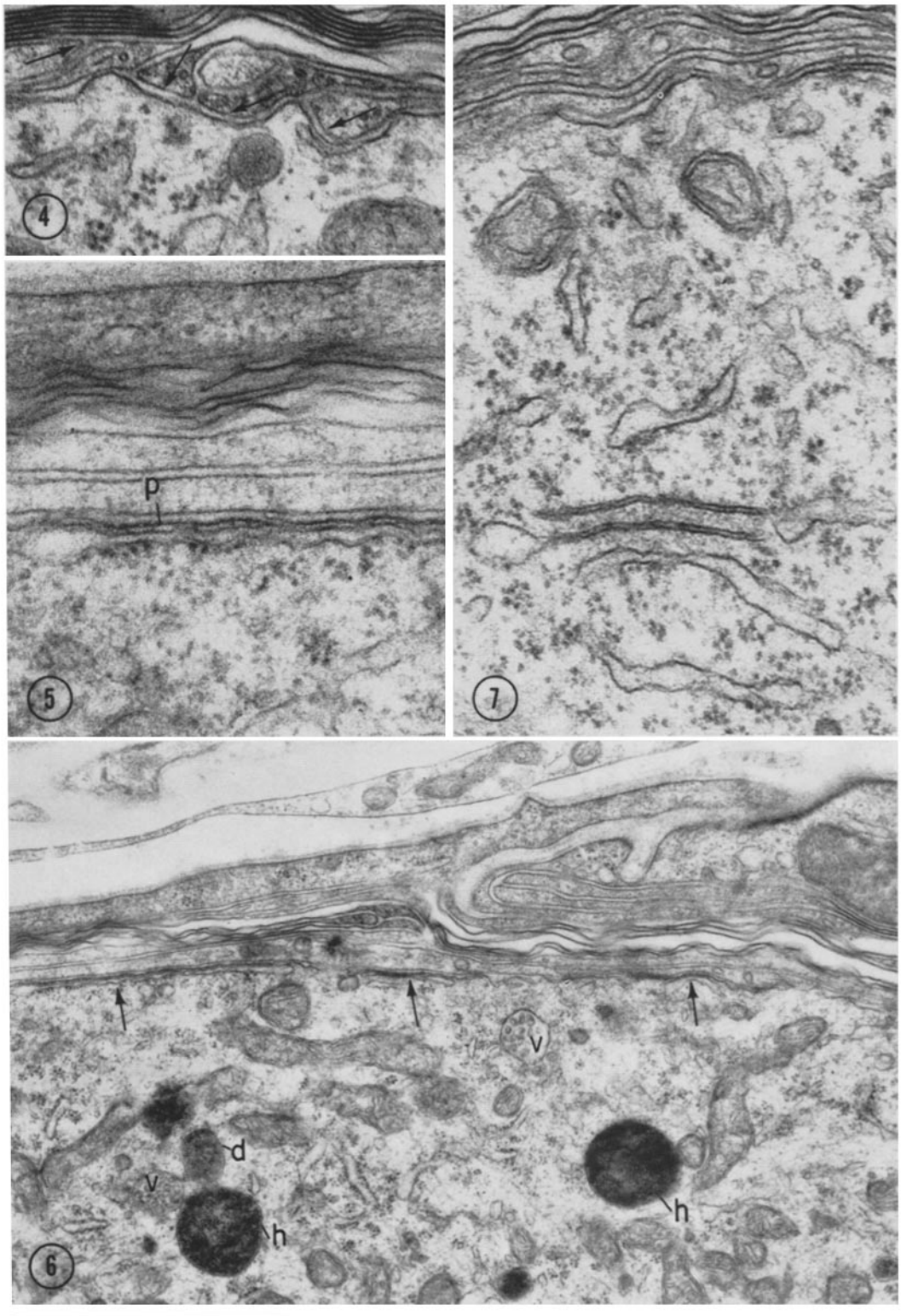
4
p
5
7
v
d
v
h
h
6

thin. The other cells present in Fig. 2 are of the type shown in Fig. 1. Fig. 3 is a higher magnification electron micrograph of these two types of ganglion cells. The cytoplasm of the cell on the left appears dense because of the high concentration of ribonucleoprotein (RNP) granules between the cisterns of endoplasmic reticulum. Very few neurofilaments are to be seen, however. In contrast, the cell on the right exhibits a large area in which there are few RNP particles, but a high concentration of neurofilaments and fine tubules, the majority cut transversely.

Both types of cells exhibit inclusion bodies of several types. In addition to the familiar granular bodies (*d* in Fig. 3) and multivesicular bodies (*v* in Figs. 3 and 6), there are also larger, heterogeneous bodies containing granular material of varying density, as well as irregular membranous components (*h* in Fig. 6). These resemble lysosomes, which have been described in numerous cell types.

A fourth type of inclusion is shown in Fig. 10 (*i*) in the region of the Golgi membranes. It consists of granular material of intermediate density, and is not limited by a membrane. Large, stellate, homogeneous, dense inclusions resembling lipid deposits are also occasionally encountered. They are not illustrated here.

Two modifications of the endoplasmic reticulum in these neurons warrant special mention. First are the subsurface cisterns, which are flattened against the neuronal plasmalemma and separated from it by a light zone of less than 100 A. Figs. 5 and 6 show examples of this, one of which (at the left of Fig. 6) is 2 μ long. Ribonucleoprotein particles adhere to its deep surface. These structures are common in cells ensheathed by thin loose myelin, but are only occasionally encountered in cells ensheathed by compact myelin. The second modification is illustrated in Fig. 7. It consists of two markedly flattened cisterns removed from the surface of the neuron. They are separated from each other by an interval of ~400 to 500 A, which contains fine granular material of intermediate density. A third cistern which is not so compressed is adjacent to the other two with the same kind of granular material intervening. No ribosomes lie between these cisterns. This modification of the endoplasmic reticulum bears some resemblance to the "spine apparatus" described by Gray (13).

Perikaryal Sheaths

A. Types of Myelin

Perikaryal myelin in the rat is in some cases typically compact, but more commonly exhibits some degree of incompactness, such as occurs in

FIGURE 8

Compact myelin sheath over a cochlear ganglion cell. The Schwann cell nucleus is at the left. The perinuclear cytoplasm contains Golgi membranes, a heterogeneous inclusion body, many globular mitochondria which have dark granules associated with their cristae, and granular endoplasmic reticulum. A basement membrane coats the outer surface of the Schwann cell plasmalemma. Seven compact and one semicompact lamellae lie between the Schwann cell cytoplasm and the neuronal plasmalemma. × 29,000.

FIGURE 9

Loose myelin sheath over a cochlear ganglion cell. At the left side of the figure only the second and fourth lamellae from the outside appear as major dense lines. The others all contain cytoplasm including vesicles, small inclusion bodies, RNP particles, and fine granular material. Many of the lamellae terminate in this field (arrows). × 31,000.

FIGURE 10

Another part of the same neuron shown in Fig. 9. Here the sheath consists of only a single layer of Schwann cell cytoplasm at the left of the figure, in contrast to a maximum of fifteen lamellae in Fig. 9. The outermost layer of this sheath makes a U-turn around two blind loops near the left side of the figure. An external mesaxon occurs at the extreme right. At the bottom of the figure there is a collection of Golgi membranes in the neuron, among which is a granular inclusion (*i*) having no limiting membrane. × 21,000.

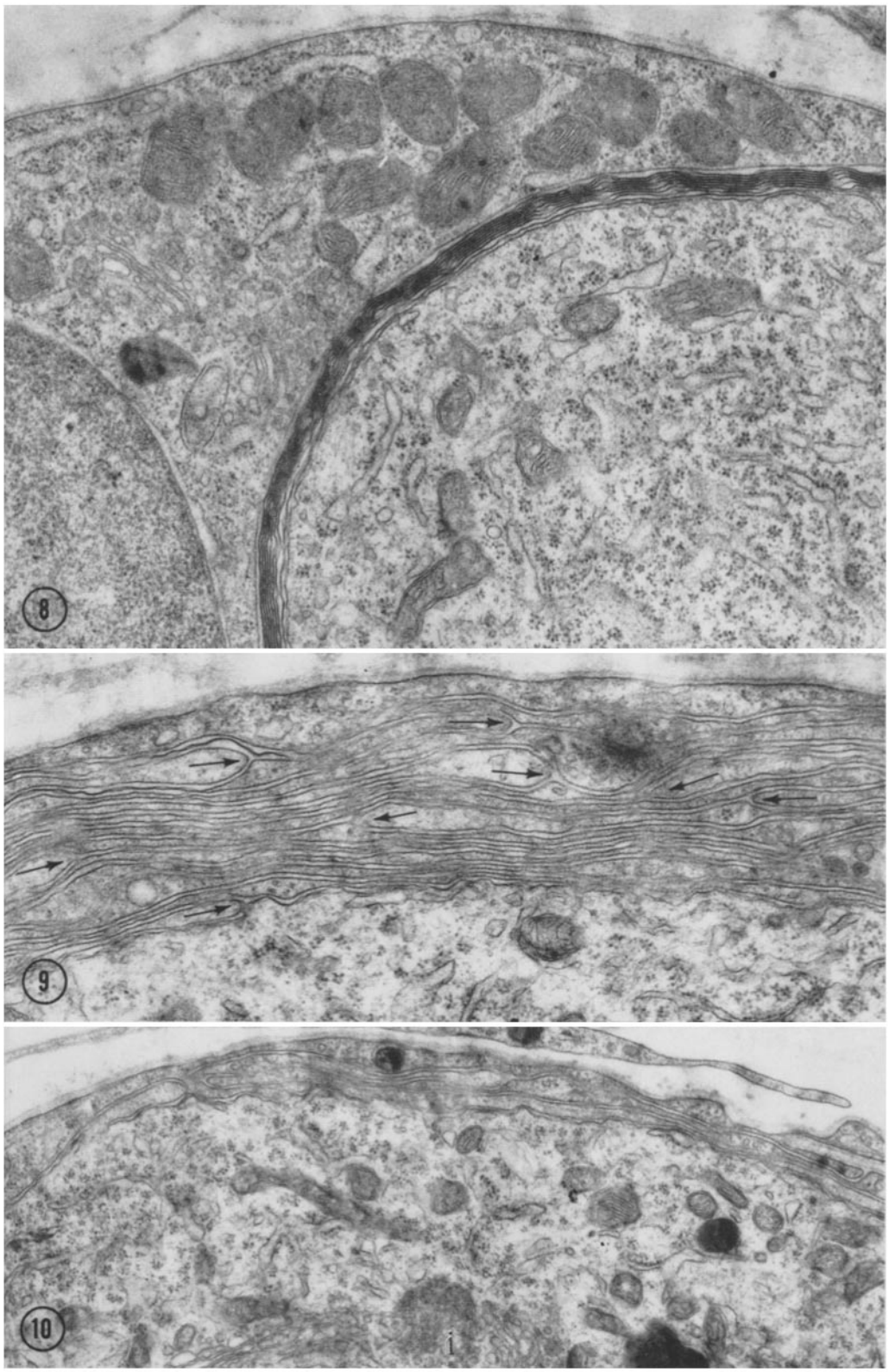
8
9
10

invertebrate nerve sheaths (14, 16), in embryonic myelin (11, 35), and in the sheaths of acoustic ganglion cells in the adult goldfish (38).

Like peripheral nerve myelin, perikaryal myelin is a layered structure which in its compact form consists entirely of membranes, and in its loose form contains Schwann cell cytoplasm as well. In the descriptions that follow, the basic structural unit of loose perikaryal myelin (one layer or lamella) will be considered to consist of a sheet of Schwann cell cytoplasm and the two cell membranes between which it lies. In the case of compact or semicompact perikaryal myelin, cytoplasm is absent and the counterpart lamella consists of the two Schwann cell membranes united along their cytoplasmic surfaces. In electron micrographs of compact myelin each such lamella is represented by one major dense line plus half the width of the light zone on each side of it.

Fig. 8 shows part of a perikaryal sheath which consists (from outside inward) of a layer of Schwann cell cytoplasm containing the nucleus, seven lamellae of compact myelin with a periodicity of ~150 A, and finally another major dense line which is separated from its neighbor by a wider light zone. Although it is not apparent at this magnification, intermediate lines occur between some of the lamellae. This sheath is, therefore, an example of thin compact myelin closely resembling that shown in Fig. 31 around an axon. Sheaths of this type are uncommon around cell bodies.

The extreme variant from this basic pattern is illustrated in Fig. 9, where nearly all the layers in the sheath contain Schwann cell cytoplasm in small amounts. Because several of the lamellae come to an end in this particular section, the number of lamellae in the sheath varies from fifteen at the extreme left of the figure to eleven in the

FIGURE 11

Sheath of a cochlear ganglion cell. At the upper right of the figure the outermost layer of the sheath bulges out and incorporates many mitochondria and RNP granules. An attenuated sheet of cytoplasm extends from this expansion downward toward the lower left of the figure. Basement membrane and interstitial space (*is*) intervene between this sheet and the sheath proper. × 13,000.

FIGURE 12

Sheath of a cochlear ganglion cell. At the right side of the figure the third lamella from the outside appears as a major dense line. At *a* it is continuous with a thick cytoplasmic layer which contains three large vesicular structures whose limiting membranes are doubled in some places. This lamella forms a major dense line again at *b*. At *c* the second lamella also splits to enclose cytoplasm. × 31,000.

FIGURE 13

Sheath over the initial portion of the axon of a cochlear ganglion cell. The sheath consists of eighteen lamellae, most of which are semicompact. Two blind loops facing each other occur in the third lamella from the axon. The axolemma is in close apposition to the sheath at the arrow but widely separated from it to the left of this region. × 58,000.

FIGURE 14

Sheath of a cochlear ganglion cell. The seventh lamella from the outside appears as a major dense line at the left of the figure. Traced to the right, it incorporates cytoplasm and then ends as a blind loop. The arrow indicates an external mesaxon. Several of the loose lamellae contain dense granular material; the outermost lamella contains many globular mitochondria. × 26,000.

FIGURE 15

Sheath of a cochlear ganglion cell. The nuclei of the two Schwann cells which form this sheath lie adjacent to each other. An elongated external mesaxon separates the cytoplasm of these two cells. The perinuclear cytoplasm of the Schwann cell at the left is packed with mitochondria, some of which display dark granules among their cristae. × 20,000.

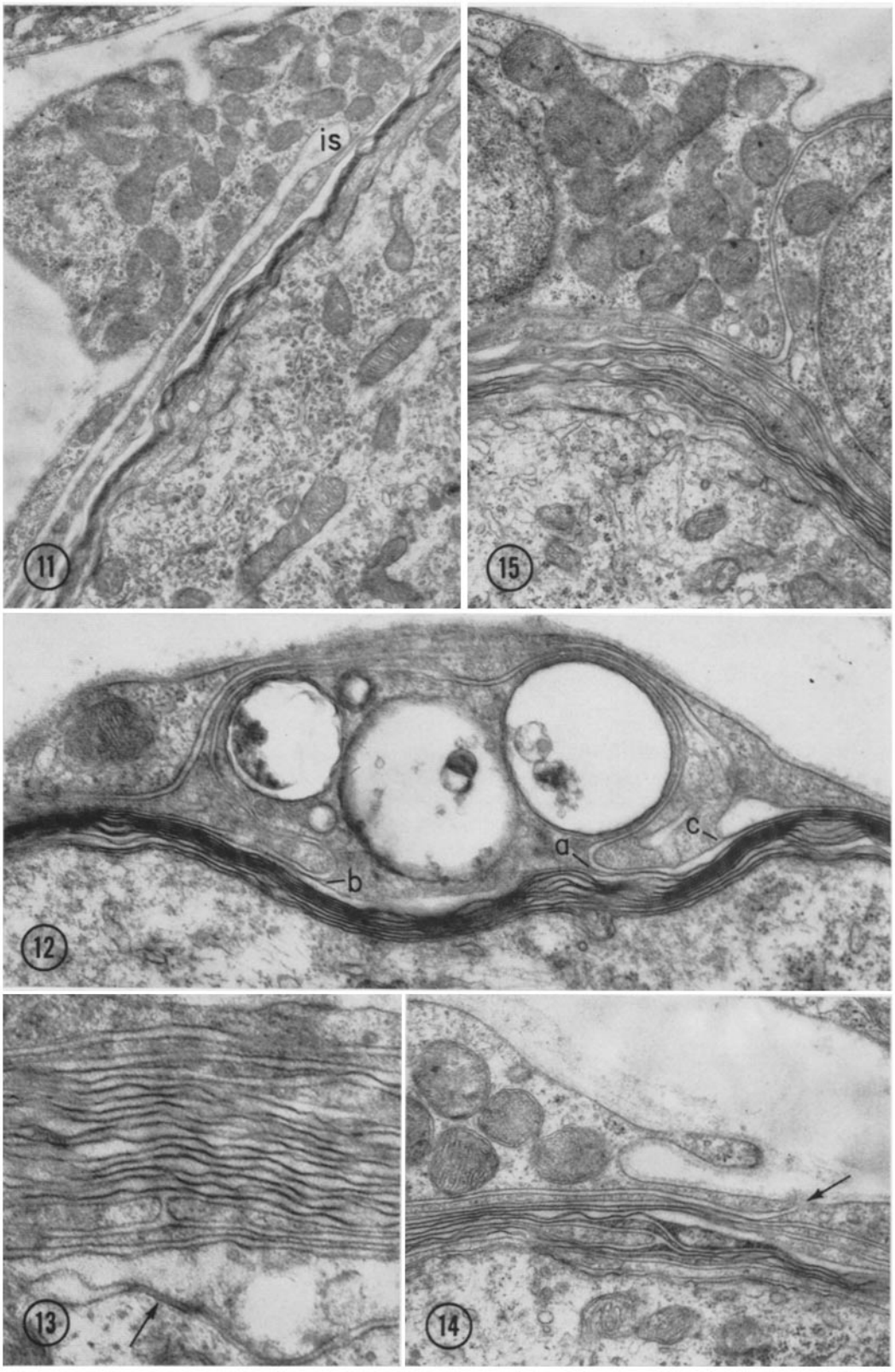
is
11
15
a
b
c
12
13
14

central part to thirteen at the right end. Although there is considerable variation in the widths of these loose lamellae, the light zones between them are relatively uniform.

Between these extremes of compact and loose myelin is an intermediate type which is illustrated in Figs. 13 and 35. Lamellae of this type appear as major dense lines containing no cytoplasm. They are, however, not completely compact. Their periodicity is ~300 A—twice that of compact myelin. As can be seen at a glance, the light zones between the major dense lines are wider than in compact myelin and contain no intermediate lines. Although the wavy appearance of the dense lines and the variations in the distance between them may be due to shrinkage during the preparation of the tissues, the over-all increase in the spacing of these lamellae, as compared with compact myelin, is probably not artifactitious in view of the typically compact appearance of adjacent myelin sheaths (as in Fig. 33). This intermediate form of myelin will be referred to as semicompact.

Generally a single perikaryal myelin sheath contains at least two of these three types of myelin in varying proportions over the surface of the neuron. It would therefore be inaccurate, strictly speaking, to characterize a given perikaryal sheath as "compact" or "loose." There is usually a predominance of one type, however, so that at low magnification the sheaths appear to be more or less homogeneous. Fig. 3 shows two adjacent neurons whose sheaths demonstrate this point. The sheath at the left consists of both loose and semicompact lamellae, and the sheath at the right includes all three types. Unlike perikaryal sheaths in the goldfish, those in the rat all have a relatively small number of lamellae, ranging from one to about twenty (average about ten). The type of myelin which predominates in a sheath is not related to the number of lamellae in that sheath.

B. Sheath Cell Cytoplasm

With the exception of the outermost layer of a sheath, loose lamellae generally contain only smooth surfaced vesicles and fine granular material which is less dense than RNP particles. Occasionally, as in Fig. 12, one layer widens considerably and incorporates one or more large, vesicular inclusion bodies.

Desmosomes also occur between loose lamellae either singly or in stacks. In the goldfish the desmosomes in loose perikaryal sheaths exhibit not only an accumulation of amorphous, osmiophilic material on their cytoplasmic sides, but also three dense lines parallel to the cell membranes in the space between the lamellae (38). No such complex structure is present in the rat, however. Only the cytoplasmic densities and widening of the interlamellar space occur. In Fig. 36 an example of a stack of desmosomes is shown between the cytoplasmic loops of the Schwann cell at a node of Ranvier.

The outermost layer of a perikaryal myelin sheath differs from all the others. It always contains Schwann cell cytoplasm, and its outer surface, which faces the pericapillary space, is always covered by a basement membrane. It is in this layer that the Schwann cell nucleus and centriole are located. There is strikingly dense packing of granular endoplasmic reticulum, Golgi membranes, and mitochondria in this layer. Indeed, the concentration of organelles here often appears to be higher than in the subjacent neuron (as in Fig. 8). It is striking, too, that the mitochondria not only are more closely packed together but also are different in configuration from those in the neuron (Figs. 11, 14, 15). Their profiles tend to be round rather than elongated, and they contain dense granules associated with their cristae comparable to those described in renal (26, 30) and intestinal (26, 53) epithelia. (It has been suggested (53) that intramitochondrial granules are especially prominent in cells engaged in the transport of water and ions.) Although aggregates of mitochondria usually occur in the perinuclear region of the Schwann cell, they can also be found in crescent-shaped expansions of the outer Schwann cell layer at some distance from the nucleus (Figs. 11, 14).

The apparently rich endowment of the Schwann cell cytoplasm with mitochondria is consistent with previous histochemical observations (29, 54) suggesting that the satellite cells of peripheral ganglia have a high oxidation-reduction activity. It should be borne in mind, however, that the outermost layer of Schwann cell cytoplasm in a loose myelin sheath represents only a part of the total cellular volume, the rest being contained in the remaining lamellae of the sheath. If the mitochondria were distributed uniformly throughout this volume, their concentration would undoubtedly appear much less impressive.

One of the characteristics which the free surfaces of these Schwann cells share with those of satellite cells in the dorsal root ganglion (37) is their tendency to extend long, thin processes running parallel to the neuronal surface. This characteristic is illustrated in Fig. 11, where the outermost layer of the sheath bulges out to incorporate an accumulation of mitochondria and RNP granules. An attenuated extension of this protuberance doubles back over the surface of the sheath. Note that the reflected basement membrane and a thin cleft of extracellular space intervene between this extension and the sheath proper.

The sheath may also buckle and fold on itself as if too large for the subjacent neuron (Fig. 16). Instances of this type of folding occur most frequently in sheaths which are composed largely of compact myelin. They are comparable to the outpouchings of myelin sheaths described by Webster and Spiro at nodes of Ranvier (52).

C. Discontinuities in Perikaryal Myelin

Unlike the myelin sheaths of peripheral nerve fibers, perikaryal sheaths exhibit lamellar discontinuities and irregularities of several types. The one encountered most frequently consists of a lamella which ends as a blind loop of cytoplasm in the middle of a sheath rather than at an external or internal mesaxon.[1] A typical example is shown in Fig. 14. The perikaryal sheath in this instance consists of ten lamellae at the left side of the figure but only eight lamellae at the right. The reason for the disparity is clear. The outermost lamella ends at the origin of an external mesaxon, and in addition, the seventh layer from the outside, at the left, ends as a blind loop oriented in the same direction as the external loop. This lamella appears as a major dense line throughout most of its length, but encloses cytoplasm shortly before it terminates. In another instance (Fig. 13), two lamellae end as blind loops facing each other with no change in the total number of lamellae in the sheath. Examples of this type are uncommon.

A much more striking example of blind endings is illustrated in Fig. 9, where no less than eight terminations can be counted (arrows). Some of these occur in adjacent layers, but others are separated by lamellae which are continuous across the field.

A second manifestation of irregularity is illustrated by Fig. 10, which shows a nearby portion of the same neuron shown in Fig. 9. At the extreme left of this figure, the sheath over the neuron consists of only one Schwann cell lamella in contrast to a maximum of fifteen lamellae in Fig. 9. Although this is an extreme and unusual example, instances of smaller variations in the number of lamellae in the sheath of a single neuron are common.

A third form of irregularity is illustrated in Fig. 6. At the extreme right side of the figure the outermost layer in the sheath accompanied by its basement membrane dips under a flap of cytoplasm coming from the left, and, after a short distance, makes a U-turn around two blind loops. Its further course is back toward the right side of the figure. In other words, this one lamella changes its direction in the figure.

In other instances many lamellae in a sheath double back on themselves in a similar manner. In Fig. 17, for example, the myelin sheath surrounding the right half of the cell is considerably thicker than that on the left. At a higher magnification (not shown) it can be seen that the thick part of the sheath consists of seventeen lamellae, and the thin part of only seven. The disparity arises because at the arrow several lamellae coming from the right side of the figure terminate, and in addition several others reverse their direction and continue back toward the right. Fig. 18 shows a more striking example of this phenomenon at higher magnification. At the top of the figure the second layer from the neuronal surface bifurcates and encloses eleven lamellae which reverse their direction, plus three others which terminate as blind loops. The mode of development of sheaths of this kind is obscure, although one plausible possibility is that they arise by way of the kind of buckling illustrated in Fig. 16.

A fourth type of irregularity encountered in these sheaths is illustrated in Fig. 23. Here both inner and outer mesaxons are clearly shown. However, the terminal loops of cytoplasm adjacent to them are facing in the *same* direction, instead of oppositely as would be expected from a simple helix. On closer examination there also appear to be two blind loops next to each other in the middle of this sheath, again oriented in the same direction, but oppositely to that of the inner and outer loops.

[1] Although the term mesaxon was originally coined to apply to axonal sheaths (9), it will be used here in describing perikaryal sheaths, for the sake of convenience.

In many cases a perikaryon or its immediately adjacent neurite is surrounded by a sheath in which more than one external or internal mesaxon can be identified. In Fig. 21, for example, arrows indicate that the extracellular space enters this sheath through *two* channels, *i.e.*, there are two external mesaxons. In Fig. 22 the outermost lamella of this sheath traced from its bulbous external origin makes one complete turn around the axon and then, just beyond the origin of the two mesaxons, it becomes the third layer in the sheath rather than the second. The second layer interposed between them is entirely separate. Unfortunately the further course of these lamellae is obscure because of obliquity of their membranes in several areas. Fig. 29 shows another example of two external mesaxons in the same sheath. Fig. 4 illustrates what appear to be multiple internal mesaxons.

Another instance of multiple mesaxons, in this case in the sheath surrounding a cell body, is illustrated in Fig. 19, which is a diagram derived from several serial montages. A low power electron micrograph of one of these sections is shown in Fig. 20, and two details at higher magnification in Figs. 24 and 25. In the original montages it is possible to follow the lamellae of the sheath, in their course around the neuron, from the innermost to the outermost layers. Although it was not feasible to reproduce the original montages because of their large size, the observed interrelationships of the components of the sheath are presented diagrammatically in Fig. 19, and are referred to in the descriptions of Figs. 24 and 25.

This sheath is noteworthy in two respects: it has two external mesaxons, which are at opposite sides of the perikaryon, and it is composed of lamellae which clearly arise from at least two separate Schwann cells, both of whose nuclei (*S1* and *S2* in Figs. 19 and 20) are visible. Components from each of these cells can be traced into the sheath, and, as is indicated in the diagram, these lamellae interleave and alternate with each other in their course around the cell body. A third spiral, whose origin is shown at *x* in Figs. 19 and 25, also interleaves with the first two in making its one turn around the cell. The sheath is further complicated by the presence of a number of "abortive" lamellae, immediately adjacent to the neuron, which traverse only a small portion of the neuronal surface and then end. In one region five such lamellae overlap one another, resembling the sheath at a node of Ranvier.

Figs. 24 and 25 are higher magnifications of the boxed areas in Fig. 20, showing the two external mesaxons present in this sheath. At this magnification individual lamellae can be distinguished. In Fig. 24 the sheath consists of seven lamellae at the top of the figure and eight at the bottom. The first lamella, immediately adjacent to the neuron, is an abortive one which does not completely encircle the neuron. The second lamella belongs to

FIGURE 16

Sheath of a cochlear ganglion cell. Most of the lamellae in the sheath fold on themselves to produce a convolution. One component of the sheath (*s*) appears to be isolated from the remainder, but is probably continuous with it in another plane. × 27,000.

FIGURE 17

Cochlear ganglion cell. The sheath over the right half of this cell is clearly thicker than that over the left half. At the arrow several layers from the right half double back on themselves, and several others terminate. The loose outermost lamellae are separated from the compact lamellae by a shrinkage space. Many areas of the neuronal cytoplasm contain only neurofilaments (*cf.* Figs. 2 and 3). × 5,000.

FIGURE 18

Sheath at the axon hillock of a cochlear ganglion cell. Neuronal cytoplasm is at the left. At the top of the figure, the second lamella from the neuronal surface bifurcates (arrows) and surrounds fourteen additional lamellae. Three of these terminate as blind loops of cytoplasm and the remaining eleven reverse their direction in the figure. The sheath is accordingly thicker by twenty-six lamellae at the bottom of the figure than at the top. × 60,000.

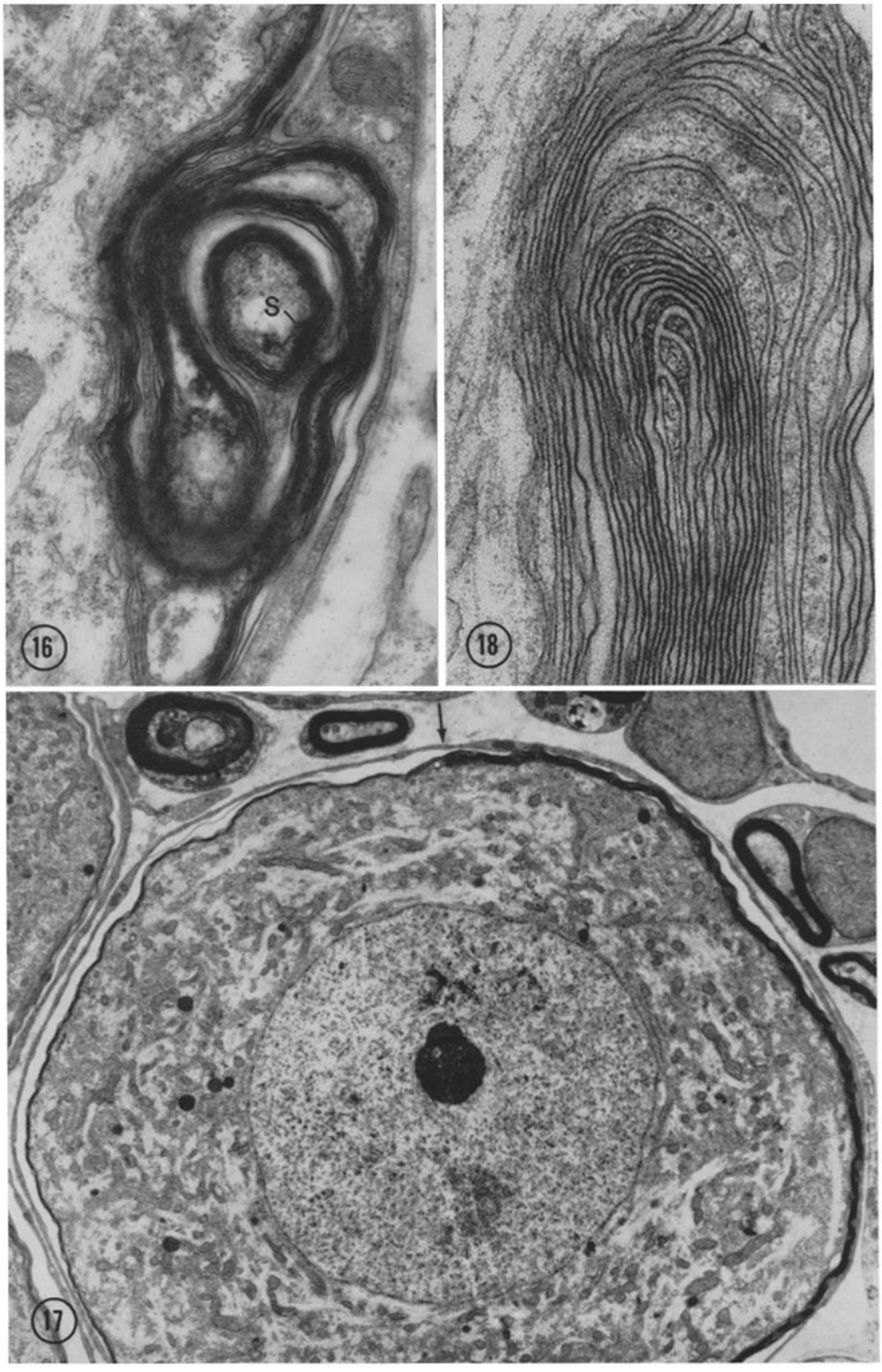
S
16
18
17

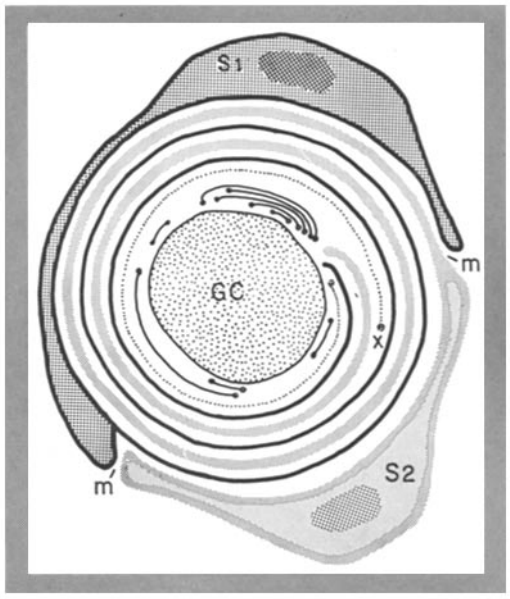

FIGURE 19

Diagram of the sheath around the cochlear ganglion cell shown in Fig. 20. The outer portion of the sheath is composed of alternating spiral lamellae from two separate Schwann cells (*S1* and *S2*). At *x* a third spiral begins and interleaves with the other two. Immediately surrounding the ganglion cell (*GC*) are several short "abortive" lamellae which do not completely encircle the neuron. The number of lamellae in the sheath varies from six to eleven. *m* indicates external mesaxons.

FIGURE 20

Cochlear ganglion cell with the nuclei of two Schwann cells (*S1* and *S2*) in its sheath. Higher magnification montages of this section and several serials of it show that both Schwann cells contribute to the sheath. Their extensions form interlocking spirals whose lamellae alternate with each other. The configuration of the sheath is shown diagrammatically in Fig. 19. Two external mesaxons lie in the boxed areas (shown at higher magnification in Figs. 24 and 25). × 3,200.

FIGURE 21

Detail of Fig. 22. Two external mesaxons (arrows) are shown in the sheath around the initial segment of an axon. Both are lined by basement membrane in this region. Interstitial space (*is*) is at the right. × 49,000.

FIGURE 22

Sheath over the initial segment of an axon. The outermost layer of the sheath can be traced from its bulbous origin (*L1*) at the right completely around the axon. After one complete turn it dips under the origin of the second layer (*L2*) of the sheath to become the third lamella from the outside. *L1* and *L2* are not connected. × 14,000.

FIGURE 23

Sheath over the initial segment of an axon. Both inner and outer mesaxons can be identified, but the terminal loops of cytoplasm adjoining them (arrows) are oriented in the *same* direction. Two other blind loops (arrows) adjacent to each other in the middle of the sheath face in the opposite direction. The axolemma closely apposes the first layer of the sheath at *a*. × 33,000.

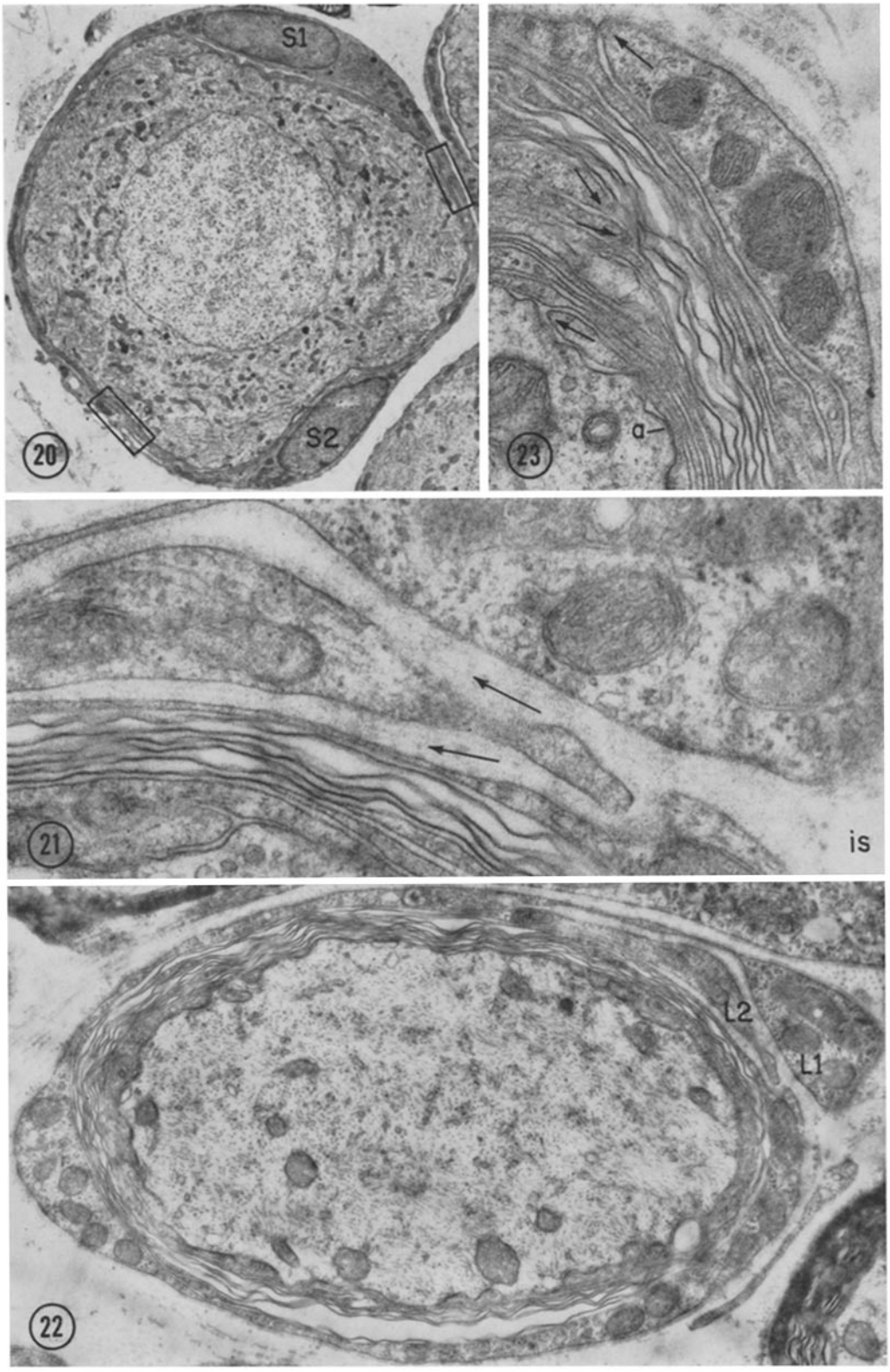
S1
S2
20
23
a
21
is
L2
L1
22

the spiral originating at *x* in Fig. 25, which makes only one complete turn around the neuron and is not connected with either *S1* or *S2* (see Fig. 19). The third, fifth, and seventh lamellae are continuous with *S1*, and the fourth, sixth, and eighth can be traced to *S2*. Correspondingly, in Fig. 25 there are nine lamellae at the top of the figure and eight at the bottom. An abortive lamella begins at the arrow and runs downward adjacent to the neuron. The layer immediately superficial to this one is part of the spiral originating at *x*. At the top of the figure, the second, fifth, seventh, and ninth lamellae from the neuronal surface are extensions of *S1*, whereas the third, sixth, and eighth lamellae connect with *S2*. The fourth lamella begins at *x*. The three interlocked spirals all come to an end in approximately the same vicinity on the neuronal surface, as indicated in Fig. 19. The overlapping pattern of their terminations is reminiscent of sheath structure at a node of Ranvier.

As can be seen in Figs. 24 and 25, lamellae are not always clearly delineated from their neighbors because of tangential sectioning. Serial sections were of some value in clarifying their paths in some cases, but not in others. Consequently some degree of interpolation was necessary in order to arrive at the diagram presented in Fig. 19. It was assumed, for example, that the second lamella on one side of a blurred area was continuous with the second lamella on the other side. Because of these technical difficulties the structure arrived at cannot be offered as a fact, but only as the most reasonable analysis of those data which are clear.

Another example of two Schwann cell nuclei in the same sheath is shown in Fig. 15, where the two nuclei are close together rather than on opposite sides of the neuron.

The final type of discontinuity encountered in these sheaths consists of the apparent fusion of two adjacent lamellae to form a single lamella. At the top of Fig. 26 the third lamella from the right is a major dense line. Traced downward, it quickly incorporates cytoplasm and becomes a loose lamella containing a chain of vesicles. At the level of *a* this single loose lamella becomes continuous with *two* major dense lines. These continue to *b*, where they are both continuous with a single layer of loose myelin containing a row of vesicles, which runs all the way to the bottom of the figure. Within this final chain there is a region of increased cytoplasmic density resembling a desmosome. Thus, in this case, a single major dense line at the top of the figure is continuous with two dense lines at the center of the figure. Accordingly, one more lamella (eight) can be counted between *a* and *b* than at the top or bottom of the figure. Fig. 27 is an enlarged detail of Fig. 26 showing one of the regions in which two major dense lines are continuous with a single loose lamella. Fig. 28 shows a detail from a different sheath. In this case a single loose lamella containing a chain of vesicles is continuous, near the top of the figure, with two *loose* lamellae, one of which terminates

FIGURES 24 AND 25

The regions of the external mesaxons indicated in Figs. 19 and 20. Alternate lamellae composing the sheath are numbered at the top of each figure.

FIGURE 24

The outermost layer of the sheath in the upper half of the figure is continuous with the Schwann cell labeled *S1* in Figs. 19 and 20. It dips under a layer which is continuous with a second Schwann cell (*S2*) and almost immediately becomes a semicompact lamella (at the arrow). *m*, external mesaxon. × 38,000.

FIGURE 25

Near the top of the figure, a tongue of cytoplasm coming from *S1* overlaps the outermost layer of the sheath (continuous with *S2*) to form the second external mesaxon (*m*). *x* shows the external origin of a third spiral which does not connect with either *S1* or *S2*. The arrow indicates the origin of an "abortive" lamella (see text) against the neuronal surface. Its limiting membrane and the neuronal plasmalemma are cut tangentially at this point. × 38,000.

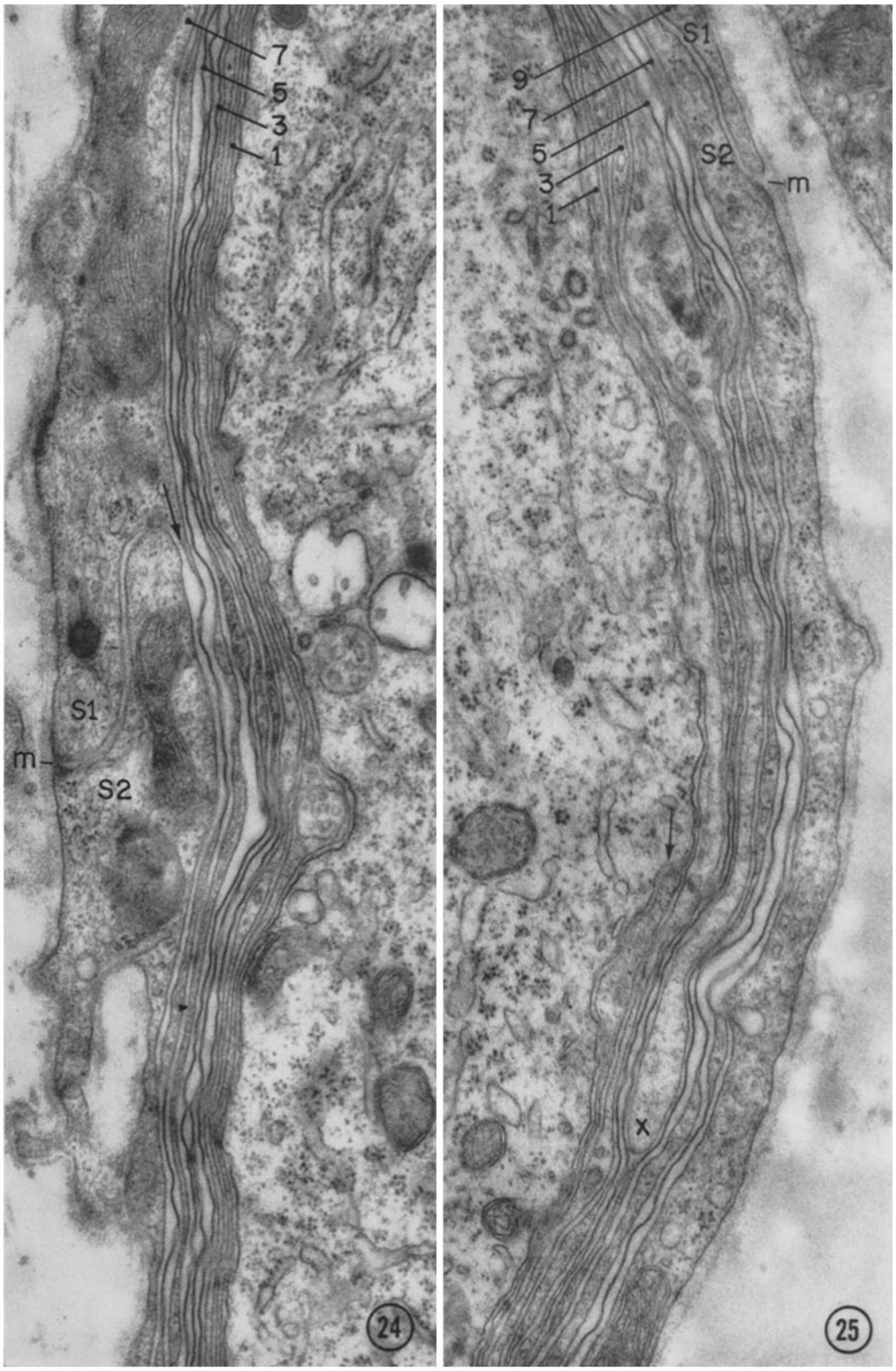
7
5
3
1
S1
m
S2
24
S1
9
7
5
3
1
S2
m
x
25

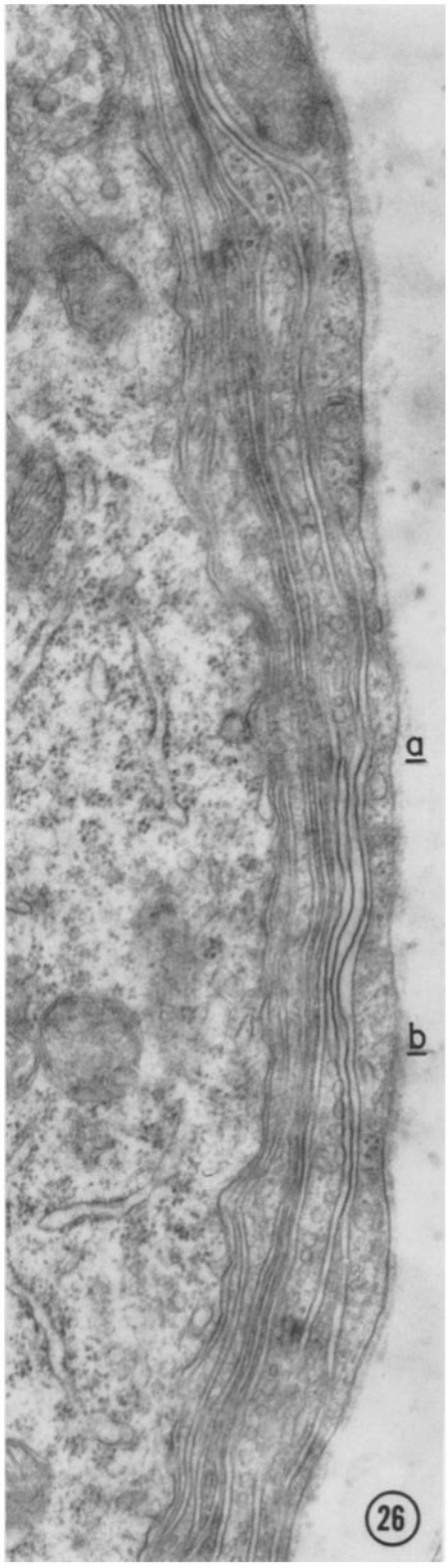

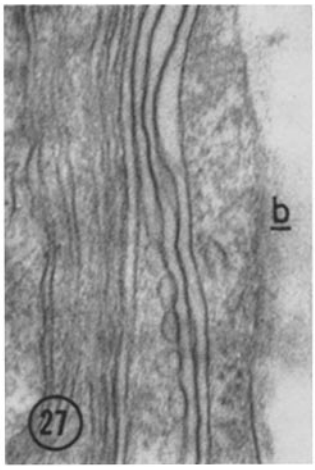

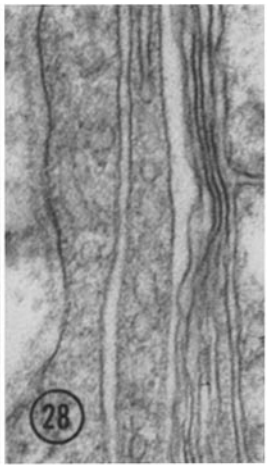

FIGURE 26

Fusion of perikaryal lamellae. At the top of the figure the third lamella from the outside appears as a major dense line. Traced downward, it incorporates cytoplasm including a chain of vesicles. At *a* it is continuous with two major dense lines, and at *b* these two dense lines are continuous with a single loose lamella containing another chain of vesicles. There are seven lamellae in the sheath at the top and bottom of the figure, and eight between *a* and *b*. × 35,000.

FIGURE 27

Detail of Fig. 26. The region of *b* is shown at higher magnification. The space between the third and fourth lamellae from the right at the top of the figure appears to be continuous with the lumen of the first vesicle in the third lamella below *b*. × 60,000.

FIGURE 28

Another perikaryal sheath showing fusion of loose lamellae. The second and third lamellae from the left at the very top of the figure are continuous with a single lamella containing a chain of vesicles. × 60,000.

as a blind loop in an adjacent part of the section (not shown).

Nerve Fibers

Although attention was focused principally on nerve cell bodies and their sheaths, several observations were made on nerve fibers and nodes of Ranvier, which deserve mention. Figs. 31 and 32 show a typical myelinated nerve fiber from the spiral ganglion. Its sheath is composed of sixteen to seventeen lamellae, of which the outer three are loose in the region of the external mesaxon. In addition, the innermost lamella is a thin layer of loose myelin continuous with the cytoplasmic loop adjacent to the internal mesaxon. Where the sheath is cut obliquely, the three components of this innermost loose lamella merge into a soft blur. The periodicity of the compact lamellae is ~150 A. Only one external and one internal mesaxon are present in this sheath, and there is a constant separation between the sheath and the axolemma. The axoplasmic organelles are sparse and consist primarily of neurofilaments.

In contrast, the initial segment of an axon shown in Fig. 29 exhibits a sheath characterized by loose and semicompact lamellae, with two external mesaxons. The cleft between the axolemma and the sheath is variable in width, and the axoplasm has a relatively high concentration of organelles including many cross-sections of tubules and mitochondria.

Some unmyelinated fibers whose source is unknown were also encountered. Fig. 30 shows an example in which a single basement membrane surrounded by collagen fibers encloses two distinct units. That at the top consists of a typical unmyelinated fiber with its crinkled axolemma enclosed within one and one-third turns of a typical Schwann cell containing fine granular cytoplasm. The organization of the unit at the bottom is less clear. It probably consists of one or perhaps two small axons surrounded in an irregular fashion by several disconnected processes. The cytoplasm of these processes has a more watery appearance than Schwann cell cytoplasm, and it contains bundles of filaments (cut in cross-section), like those in glial cells. In addition, there are two regions where the cleft separating the apposed membranes of these processes narrows considerably. These regions resemble areas of close apposition of adjacent cardiac muscle cells (45), Schwann cells (38), ependymal cells (2), and bladder epithelial cells (4). Note that basement membrane bridges over all the external mesaxons shown in Figs. 29, 30, and 31.

Some of the nodes of Ranvier encountered in this study display unusual features. In addition to the occasional occurrence of desmosomes between the paranodal terminal loops of Schwann cell cytoplasm (Fig. 36), there are also deviations from the previously described (36, 48) orderly, overlapping pattern of these loops. In Fig. 37, for example, many of the myelin lamellae coming from the right side of the figure end not against the axolemma itself, but at some distance from the axon, so that not all the myelin lamellae make contact with the axonal surface in this plane. Whether or not this particular sheath represents the termination of a perikaryal myelin sheath at a primary node of Ranvier could not be determined from the section.

Several examples of the first node of Ranvier adjacent to a perikaryon were examined. As in the goldfish, the node is asymmetric. The number of layers on the perikaryal side is smaller than that on the distal side, and the layers on the perikaryal side may be wholly or partly loose, whereas those on the distal side are all compact. Figs. 33 to 35 show an example of such a node; the perikaryal side is at the bottom of Fig. 33. The length of this node is 3 to 4 μ and its diameter is 1 μ. Its surface area is ~11 μ^2—approximately the same as the surface area of an A fiber node 0.5 μ in length and 8 μ in diameter.

DISCUSSION

In several respects the rat auditory and vestibular ganglia resemble the eighth nerve ganglion of the goldfish. The cells are bipolar and accordingly form a link in the chain of segments between the peripheral receptors and the brain stem. The cell bodies in both cases exhibit myelin around their perikarya but it is generally less compact than axonal myelin. Perikaryal sheaths in both species extend over the adjacent portions of the neurites issuing from the cell bodies up to the first node of Ranvier. Beyond this interruption the neurite is invested with typical compact myelin, containing many more lamellae than the sheath over the perikaryal internode. Nerve cell bodies from the acoustic ganglia of both species are differentiated into two types: those with densely packed granular cytoplasm, and those with cytoplasm which has large

clear areas containing only neurofilaments. In general the latter type is covered by compact myelin.

Despite the over-all similarity between the acoustic ganglia of these two species, certain important differences are evident. Nerve cell bodies in the rat have a generally higher concentration of RNP particles, and their Schwann cells have a greater concentration of mitochondria, which tend to be globular rather than filamentous, and which exhibit granules among their cristae. Perikaryal sheaths in the rat are uniformly thin and show distinct discontinuities and irregularities in their lamellar structure.

The use of the term "myelin" in describing the perikaryal sheaths of either the rat or the goldfish presents a semantic problem. In peripheral nerves there is a convenient sharp structural distinction between those fibers which are myelinated and those which are unmyelinated. The former are sheathed by multilayers of osmiophilic membranes which exhibit a characteristic periodicity, while the latter are enclosed in a single Schwann cell layer which contains cytoplasm. Although some perikaryal sheaths fall clearly into either of these two categories, most of them occupy a gray area between these extremes. Such intermediary sheaths may contain semicompact lamellae consisting of major dense lines which are not in close apposition, or they may contain loose lamellae consisting of thin layers of Schwann cell cytoplasm which may or may not be in close apposition. Lamellae of these types may be continuous with each other and with lamellae of typical compact myelin. The number of lamellae may be as low as one or two, or, in the goldfish, as great as ninety. There is, unfortunately, no obvious discontinuity in the spectrum of perikaryal sheaths which can be used as a dividing line between myelinated and unmyelinated.

In this paper all perikaryal sheaths consisting of more than one layer are considered to be myelinated, regardless of the presence or absence of Schwann cell cytoplasm in them. Admittedly this arbitrary designation becomes confusing when

FIGURES 29 TO 31

Three types of nerve fibers in the cochlear ganglion.

FIGURE 29

Initial segment of an axon. The axoplasm contains many mitochondria, tubules, and filaments in transverse section. The axolemma is closely apposed to the sheath in some regions but more widely separated from it in others. The sheath consists of both loose and semicompact lamellae. Two external mesaxons are visible at the bottom of the figure (arrows). × 21,000.

FIGURE 30

Unmyelinated nerve fibers (*n*). The fiber at the top of the figure has a crinkled axolemma and contains filaments, tubules, and a mitochondrion in cross-section. It is surrounded by one and one-third turns of Schwann cell cytoplasm. In the lower half of the figure, one or perhaps two nerve fibers are surrounded in an irregular fashion by cellular processes which exhibit bundles of filaments in their cytoplasm. These processes are in close apposition in two regions (lower right). × 35,000.

FIGURE 31

Myelinated nerve fiber. The axoplasm contains filaments and mitochondria but few tubular profiles. It is surrounded by a sheath of sixteen to seventeen lamellae. The innermost and outermost edges of the Schwann cell forming this sheath are indicated by arrows. × 35,000.

FIGURE 32

Detail of Fig. 31. The axolemma (*p*) is at the left. Immediately adjacent to it is a thin layer of loose myelin, then thirteen layers of compact myelin having a period of ~150 A, and finally three layers of loose myelin externally. × 142,000.


29


n
n
n
30

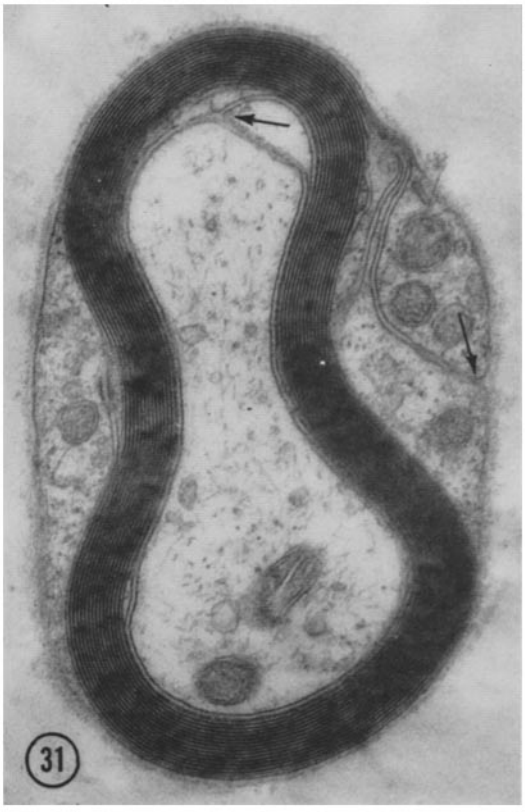
31

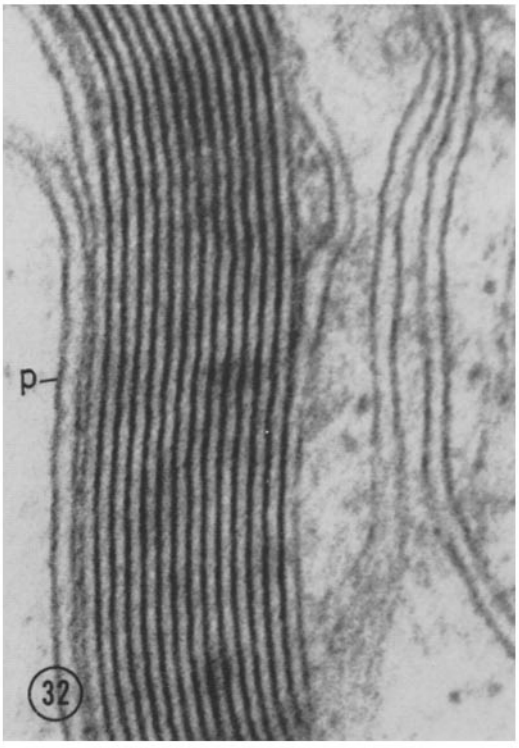
p
32

applied to sheaths in other locations. In the spinal ganglion, for example, nerve cell bodies and the initial segments of their axons are frequently surrounded by more than a single layer of Schwann cell cytoplasm; yet these structures are not generally considered to be myelinated. The problem of terminology also arises in connection with certain invertebrate nerve sheaths. This subject is discussed more fully by Schmitt (43).

The Formation of Rat Perikaryal Myelin

The lamellar structure of the perikaryal myelin sheaths examined in this study indicates that in some cases perikaryal myelin develops in a manner which differs from the simple helical formation proposed for peripheral axonal myelin (11, 31, 32). The observations supporting this are the following:

1. The number of lamellae in a given sheath varies from one region to another. Usually the difference is only a few lamellae, but in some instances (Figs. 9 and 10) it is much greater.

2. Lamellae often terminate as blind loops within the sheath. This may occur in the layer adjacent to the neuron and give rise to what looks like a typical mesaxon. However, many instances have been seen in which a single layer terminates

FIGURE 33

First node of Ranvier adjacent to a cochlear ganglion cell. The perikaryal side of the axon is at the bottom of the figure. It bears a typical perikaryal sheath consisting of sixteen lamellae, most of which are semicompact. The distal side, at the top of the figure, is sheathed by twenty-four lamellae of typical compact myelin. The node itself extends for 3 to 4 μ and is covered in part by a single layer of Schwann cell cytoplasm with its basement membrane, and in part by basement membrane alone. × 16,000.

FIGURE 34

Detail of the compact myelin sheath over the distal part of the axon shown in Fig. 33. The major dense lines split to enclose terminal loops of cytoplasm against the axolemma (*p*). × 49,000.

FIGURE 35

Detail of the semicompact myelin sheath over the perikaryal side of the axon shown in Fig. 33. The spacing of the lamellae is clearly greater here than in the compact myelin in Fig. 34. *p*, axolemma. × 49,000.

FIGURE 36

Paranodal axonal myelin sheath from the vestibular ganglion. The terminal loops of cytoplasm display a stack of desmosomes characterized by aggregations of osmiophilic material on their cytoplasmic sides, and slight widening of the interlamellar spaces. At the left of the figure, the axoplasm invaginates into the sheath. The axolemma (*p*) in this region is denser than the adjacent Schwann cell membrane. The light zone between them contains an intermediate line. A membrane-bound cistern (*c*) underlies the axolemma in this region. × 103,000.

FIGURE 37

Node of Ranvier from the cochlear ganglion. The sheath to the right of the node is distinctive in that many of its lamellae terminate at some distance from the axolemma rather than directly against it. The sheath to the left of the node does not display this characteristic. At the bottom of the figure the nodal axolemma (*p*) bulges out between the two sheaths, forming a protuberance which contains a mitochondrion and some granular material. At the top of the figure villous projections of the outermost layer of Schwann cell cytoplasm extend into the nodal region and abut against the nodal axolemma. A thin filament occurs in the center of some of these villi. Basement membrane is continuous across the node. × 29,000.

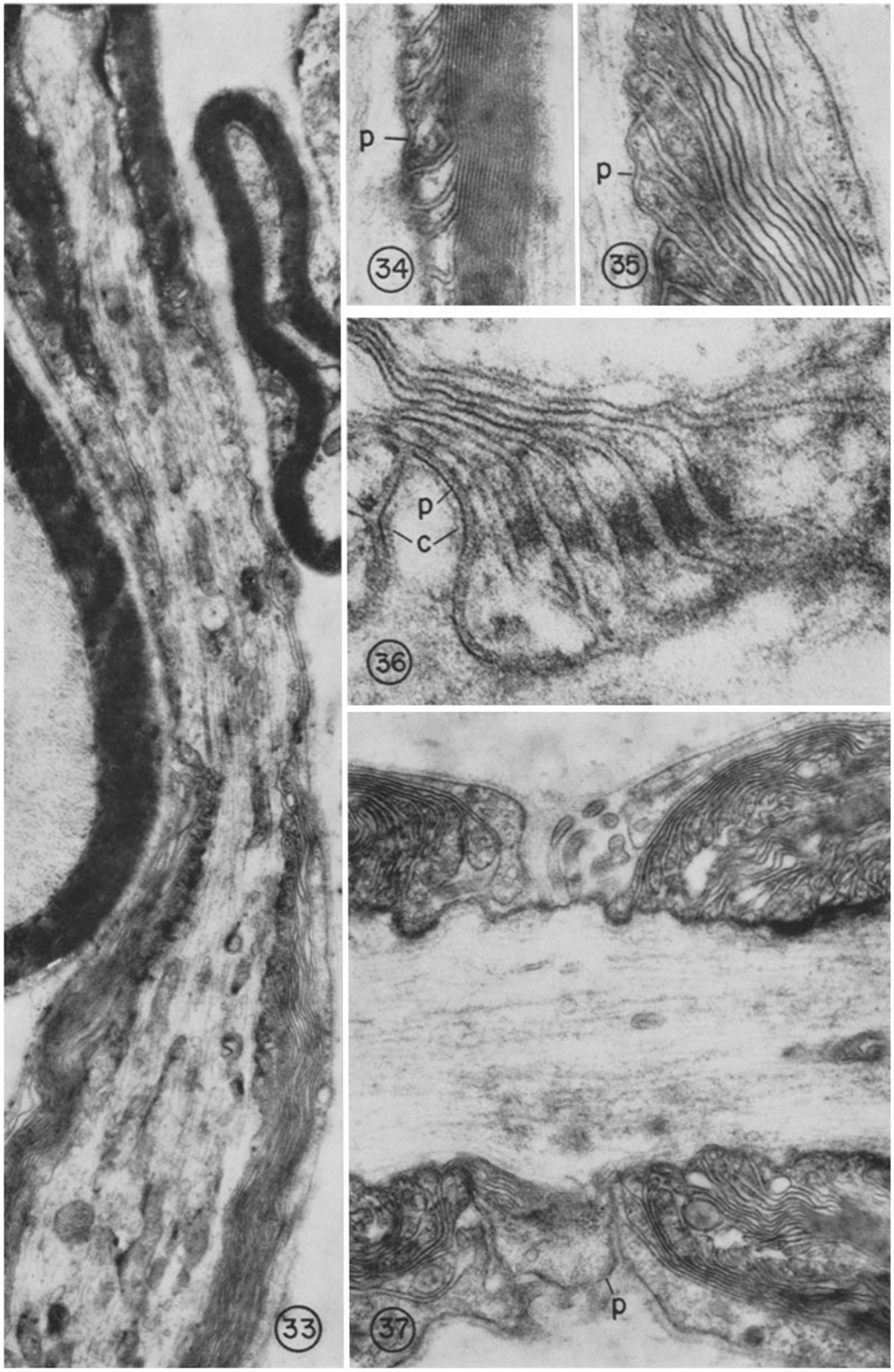
p
34
p
35
p
c
36
33
37
p

in the middle of a sheath, and not uncommonly several layers end in the same region and others continue uninterrupted.

3. Cytoplasm from two separate Schwann cells can in some cases be traced into the sheath around a single ganglion cell.

4. When the innermost and outermost edges of a sheath can be identified (adjacent to the inner and outer mesaxons), they sometimes face in the same direction instead of oppositely as in a simple helix.

5. Two adjacent lamellae may merge to form a single layer over part of their length.

6. Lamellae sometimes change direction; *i.e.*, they double back on themselves within a sheath.

Some of these observations could be accounted for by postulating multiple holes or folds in a single continuous Schwann cell sheet, and in this case a simple helical formation would not be excluded. In view of the remaining observations, however, it is clear that many of the sheaths are formed by a more complex process, which in some cases involves more than one Schwann cell.

The preceding observations suggest several possible developmental mechanisms:

1. Interlocking spirals: This pattern is depicted diagrammatically in Fig. 19. Such a sheath could develop if cytoplasmic processes from two Schwann cells advanced together around a single ganglion cell, laying down successive pairs of lamellae between the Schwann cell bodies and the neuronal surface. The advancing edges of the sheath cells would in this case have to insinuate themselves between the ganglion cell and the part of the sheath already laid down. Alternatively, processes from two Schwann cells could attach themselves to adjacent positions on the ganglion cell surface and then spiral together around the neuron with the Schwann cell nuclei in the external leading edges. The lamellae would in this case be laid down centrifugally. Rotation of the neuron would produce equivalent results. The short third spiral and the "abortive" lamellae in Fig. 19 may be connected with Schwann cells whose nuclei lie in a different plane, although it is conceivable that they represent portions of Schwann cell cytoplasm which have become detached from their nuclei.

2. Superimposed spirals: The positions of the mesaxons and blind loops in Fig. 23 could be explained if the inner six lamellae were laid down by one Schwann cell moving clockwise around the axon, and if the outer nine lamellae were subsequently superimposed on this sheath by a second Schwann cell moving counterclockwise. The outer counterclockwise portion of the sheath may not extend along the length of the nerve fiber as far as the inner clockwise portion, so that the latter could be in contact with the interstitial space in another plane.

3. Overlapping folds: Several examples are illustrated here (Figs. 6, 10, 16, 17, and 18) in which one or more lamellae in a sheath appear to fold back on themselves. The extreme cases (Figs. 17 and 18) may represent greatly prolonged evaginations or invaginations of nearly the entire thickness of the sheath. In an ideal situation, where all the lamellae in a sheath folded on themselves, it would be expected that the thick part of the sheath would contain three times as many lamellae as the thin part. The observed sheaths are not so simple, however. Evidently not all the lamellae are involved in the folding, and, to complicate matters further, several lamellae often terminate at the origin of a fold, and others bifurcate.

4. Fusion of adjacent lamellae: When the pair of cell membranes separating two lamellae comes to an end and is followed by a chain of vesicles, a question arises as to whether the vesicles are lining up and coalescing to form the membranes, or whether preexisting membranes are breaking down into a chain of vesicles. The former has been proposed as a mechanism in the genesis of myelin (5), and the latter in the disappearance of lateral infoldings of epithelial cells (28). The data presented here do not help to resolve this problem, but they do indicate that the final pattern of a myelin sheath may be complicated by either one of these processes.

It is possible that the development of perikaryal myelin may in some cases be an entirely irregular process with one or more Schwann cells sending out sheets in all directions over the surface of the neuron, which cross and overlap one another haphazardly. This would be consistent with the observation that Schwann cells characteristically thrust out attenuated projections of cytoplasm from their free surfaces as in Fig. 11. It might also account for the large variation which may occur in the number of lamellae in a single sheath (Figs. 9 and 10). Irregularities which develop in such sheaths might subsequently be "ironed out" by fusion of some of the lamellae, resulting in a transformation to a more orderly lamellar structure.

The kinds of discontinuities which have been

described do not occur in the compact lamellae of perikaryal myelin. Major dense lines have not been observed to terminate as such or to merge with one another or to bifurcate. Whenever these irregularities are observed, Schwann cell cytoplasm is always present in the lamellae concerned, even though it may extend for only a short distance beyond the site of the irregularity. This may indicate that compact myelin is able to form from loose Schwann cell lamellae only when the preexisting system is orderly. Regions of irregularity may always remain in the loose state. The fact that adult perikaryal myelin is usually not compact may then be a reflection of extensive irregularities in its lamellar structure.

Another possibility is that compact myelin may form from loose lamellae even in places where irregularities exist, but that in the transformation to the compact state these irregularities undergo a reorganization or ironing out, leaving no trace of their presence in the ultimate lamellar structure. The observation that adjacent lamellae may sometimers merge with each other lends support to this hypothesis. Perhaps fusion of this kind may also occur between the ends of two blind loops facing each other (as in Fig. 13) or between lamellae which are even more irregular, resulting in the elimination of discontinuities.

A complex developmental pattern has also been proposed for myelin in the central nervous system (23, 39), where layers from more than one glial cell may be incorporated into a single sheath in an irregular fashion. Yet adult compact myelin in the central nervous system has not so far shown evidence of this kind of irregularity. Perhaps here too an ironing out process obliterates manifestations of irregularities in these sheaths.

An embryologic study of acoustic ganglia would be necessary in order to determine whether compact perikaryal myelin develops from loose Schwann cell wrappings containing discontinuities and irregularities, or whether the different types of sheaths present in the adult animal have entirely different modes of development.

What is clear from examination of the structure of adult perikaryal sheaths is that some of them could not have been formed by the simple helical wrapping of a single Schwann cell around the neuron. The mechanics of myelination must have been more complex in these instances.

Conduction across the Perikaryon

In the acoustic nerve, ganglion cell bodies lie directly in the pathway of incoming sensory impulses, so that total conduction time for each nerve fiber from end organ to medulla will depend in part on the specific electrical properties of the segment containing its perikaryon. Direct measurements of the electrical parameters of acoustic perikarya have not been made, but it may be possible to make some inferences about them from morphologic data.

Physiologic speculation of this kind not only is relevant to auditory and vestibular nerve function, but may also have a more general application in view of the structural resemblance between some of the perikaryal sheaths discussed here and Schmidt-Lantermann clefts of myelinated nerve fibers (33), certain invertebrate nerve sheaths (14, 16), and the sheaths around other peripheral ganglion cells and their initial segments.

Among the factors which would influence conduction along the perikaryal segment are: (*a*) the resistance of the neuronal cytoplasm and the interstitial fluid, (*b*) the impedance of the perikaryal sheath, (*c*) the impedance of the neuronal plasmalemma, and (*d*) the surface area of the internode containing the perikaryon.

Resistance through neuronal cytoplasm might at first seem to be much smaller than that through axons because of the greater diameter of the perikaryon. On the basis of dimensions alone, it would be expected that the core resistance of a cell body averaging 10 μ in diameter would be roughly 25 times smaller than that of an axon 2 μ in diameter. However, the composition of the perikaryal cytoplasm is quite different from that of axoplasm. Particularly in the loosely myelinated cell bodies there is dense packing of organelles including mitochondria, RNP particles, endoplasmic reticulum, and a variety of inclusion bodies, and here the net intracellular volume which would be available for ionic flux is less than the total volume of the cell body. This consideration would be particularly important if the membranes enclosing the endoplasmic reticulum were relatively impermeable to ions. A large intracellular compartment would then be effectively closed to current flow.

Compactly myelinated perikarya generally have a smaller proportion of their total volume occupied by organelles, with sizable portions of their cytoplasm resembling typical axoplasm in

that they are nearly devoid of structured elements except for neurofilaments. It would therefore be expected that the resistance through the core of this latter type of cell would be less than that through the more densely packed cytoplasm of loosely myelinated perikarya.

The structural similarity between compact perikaryal myelin and axonal myelin is so close that it will be assumed here that they have comparable physiological effects. Tasaki (47) has calculated the ohmic resistance per unit area across frog sciatic A fiber internodes to be $\sim$100,000 ohm·cm^2. According to his estimate, these fibers measure 12 to 15 μ in diameter, of which approximately 20 to 30 per cent is composed of myelin. The periodicity of fresh frog sciatic nerve myelin is 171 A as deduced from x-ray diffraction data (7, 44). With this figure it can be calculated that the number of lamellae composing such a sheath is $\sim$100 and the resistance of each lamella is $\sim$1000 ohm·cm^2.[2] This calculation depends on the assumption that resistance across the myelin sheath is uniform along the length of the internode. If there are regions of decreased resistance, as at Schmidt-Lantermann clefts, then the calculated figure would represent only an average value, and the resistance of the compact portion of each myelin lamella would be higher.

Perikaryal sheaths consist of only $\sim$10 lamellae. If the resistance of a myelin sheath is directly proportional to the *number* of lamellae in the sheath, then it would be expected that the resistance per unit area across a perikaryal myelin sheath would be $\sim$10,000 ohm·cm^2, or about one-tenth that of the frog A fiber. (Species differences are being neglected here although the periodicity of myelin depends on the species. For example, in osmium tetroxide–fixed, Epon-embedded material, the periodicity of compact myelin in the goldfish is $\sim$115 A (38) and in the rat $\sim$150 A. This spacing difference may be correlated with a chemical and/or impedance difference.) It would similarly be expected that the capacitance of a compact perikaryal myelin sheath would be about 10 times greater than that in the frog A fiber per unit area.

However, the surface area of a perikaryal internode is probably at least 10 times smaller than that of the A fiber internode. An A fiber internode 12 to 15 μ in diameter and 2 mm in length has a surface area of $\sim$80,000 μ^2. The myelinated perikaryon shown in Fig. 2 has a surface area of only $\sim$3000 μ^2. The neurite which issues from it is only 6 μ in diameter. Assuming that the initial segments of both neurites have this same diameter throughout their length, the combined length of both initial segments would have to be more than 250 μ for the total surface area of this perikaryal internode to be 10 per cent of that of the A fiber. The first node of Ranvier has been observed to be much closer than that to the perikaryon, as in Fig. 1, where it lies at a distance of only 12 μ.

Thus the thinness of the compact perikaryal myelin sheath is probably compensated for by a corresponding decrease in internodal surface area, so that the total resistance of this sheath is no smaller than that of the A fiber myelin sheath, and the total capacitance no greater. Consequently most of the action current would be expected to flow through the nodes on either side of the perikaryal segment. The increased capacitance per unit area of the perikaryal sheath would, however, be expected to reduce the velocity of spread of the action potential along this segment (18), with the result that conduction velocity should decline in this region.

Loose myelin sheaths may have somewhat different physiological properties. Like the compact sheaths, they consist of multilayers of membranes which are partly lipoidal and which would, therefore, be expected to resist ionic current flow and to be polarizable. Each lamella of loose myelin is composed of *two* Schwann cell membranes enclosing a thickness of Schwann cell cytoplasm. It is important to note that a compact lamella is derived embryologically from *two* Schwann cell membranes (35). Thus a compact myelin sheath of ten lamellae is derived from the same number of Schwann cell plasmalemmas as a loose myelin sheath of ten lamellae, and both sheaths should have the same content of membrane lipid. In this respect compact and loose myelin are comparable.

Several differences between them are apparent, however. First of all, loose myelin contains substantial amounts of Schwann cell cytoplasm within the lamellar system, resembling the structure of Schmidt-Lantermann clefts in this regard. This cytoplasm would be expected to have relatively high conductivity as does cytoplasm elsewhere,

[2] This value was previously calculated to be $\sim$ 600 ohm·cm^2 (17). However, this calculation was based on an estimated lamellar thickness of 80 A. If the value 171 A is substituted, the calculated resistance becomes $\sim$ 1350 ohm·cm^2.

and consequently it should have no significant effect on the capacitance of the Schwann cell membranes, and should add but little to the resistance across the sheath. However, if there were a continuous thickness of Schwann cell cytoplasm leading from the outermost to the innermost layer of a sheath, a shunt pathway for current flow would be provided by the low resistance Schwann cell cytoplasm. In order to follow this channel, the current would have to traverse the Schwann cell membrane only twice, regardless of the number of layers in the sheath—once at its point of entry into the cytoplasm, and once at its point of exit. In sections it is rare to find a sheath in which all the layers are entirely loose. Usually semicompact lamellae replace loose lamellae over short stretches, so that continuity of the Schwann cell cytoplasm is interrupted at least in the plane of the section. A three-dimensional view of the sheath might nevertheless demonstrate cytoplasmic continuity in other planes, so that a low resistance current pathway through the Schwann cell cytoplasm remains a possibility.

Second, it is possible that in the course of embryological development of compact myelin from Schwann cells, the lipids of the cell membranes undergo changes. The lipid layers of adult compact myelin may therefore not be identical with those of the Schwann cell membranes from which they are derived. Accordingly, compact myelin may differ from loose myelin with respect to the chemical composition, molecular organization, and dielectric properties of its lipid component, with a consequent difference in the electrical properties of the two types of sheath.

A third difference between the electrical properties of loose and compact myelin sheaths lies in the dimensions of their interlamellar spaces. Except in the region of Schmidt-Lantermann clefts, these spaces are probably completely obliterated in compact myelin (35) (although potentially present, as has been demonstrated by soaking myelin in hypotonic solutions (34)). But in loose sheaths these spaces are present and may constitute a significant shunt pathway for ionic current flow.

Channels of this kind which connect the neuronal plasmalemma with the extracellular space also occur in the sheaths of squid giant axons (12, 49), where their path length is relatively short ($\sim$4 to 5 μ (50)). It has been suggested that a large proportion of the ion flux between the axon and the extracellular space occurs through these channels (8, 49). The resistance of squid giant axon sheaths has been estimated to be less than 5 ohm·cm^2 (8).

In the Schmidt-Lantermann clefts of myelinated nerve fibers such channels or gaps also occur but have a much greater path length around the axon (in one case estimated to be $\sim$2500 μ (33)) and in addition have a much smaller longitudinal extent. Consequently, it has been postulated that the ionic current which would follow this pathway is negligible (33).

In loose myelin sheaths the interlamellar spaces are intermediate between these two extremes. They may extend the entire length of the sheath in the same manner as the mesaxons of unmyelinated nerve fibers, although whether or not they are wide open all the way from their external openings down to the level of the axolemma is uncertain. The path length of such a channel would be $\sim$50 to 100 μ around the initial portion of an axon immediately adjacent to the perikaryon, and several times greater around the perikaryon itself. No information is available about the content of these channels or about the adsorptive properties and charges of the membranes lining them. The influence of the basement membrane which bridges over their external openings is also unknown.

Thus it is possible that in loose myelin there are significant low resistance pathways through the sheath, diminishing its effectiveness as an ionic insulator. A considerable decrement in action potential may accordingly occur along this internode, although the safety factor at the adjacent node of Ranvier is probably great enough so that nodal excitation would still occur. A partial conduction block might, however, occur with high frequency stimulation.

The remaining consideration concerns the electrical properties of the neuronal plasmalemma. Although no numerical estimate of neuron membrane impedance can be made from the structural data presented here, a relative difference between the cell membranes of loosely myelinated and compactly myelinated neurons might be anticipated. Both cell types exhibit subsurface cisterns, as illustrated in Figs. 5 and 6. These structures lie in such close proximity to the cell membrane that they may have a considerable effect on the permeability characteristics of that part of the plasmalemma with which they are associated. A relative difference in the number of these "patches" in the two types of ganglion cells might

therefore be reflected by a difference in the over-all electrical properties of their cell membranes. These cisterns are in fact encountered much more frequently in loosely myelinated than in compactly myelinated cells. They have also been described in hair cells of the organ of Corti (6) and in spinal ganglion cells (37), and have been seen in neurons of the central nervous system as well.

Significance of Two Populations of Ganglion Cells

In 1902 Kaplan (20) reported that the axoplasm of myelinated nerves could be distinguished from that of unmyelinated elements through the use of a differential stain with an anthracene blue base. Scharf (40, 41) later applied the same technique to acoustic ganglia and reported comparable results, *i.e.*, that cell bodies which were surrounded by myelin stained blue, while those which were unmyelinated took up the counterstain only. On the basis of this work it appeared that there were two groups of neurons in this ganglion which could be distinguished by their sheath characteristics and also by their cytoplasmic staining properties. The present study likewise demonstrates the existence of two morphologic types of cells in the acoustic ganglia, which differ along the same general lines as indicated by Scharf but with considerable overlap between the two groups. The distinction may be idealized as follows:

The cytoplasm of the filamented neurons has a reduced concentration of ribonucleoprotein granules, but many neurofilaments. Subsurface cisterns are uncommon. The surrounding sheath, although thin, is composed largely of compact myelin. In contrast, the granular neurons are densely packed with Nissl substance but contain few neurofilaments; subsurface cisterns are more common, and the sheath consists largely of loose myelin. Presumably the second type is the one which Scharf considered to be unmyelinated, for in the light microscope the sheath is frequently not distinguishable.

One possible interpretation of these two cell types is that they are "dark" and "light" cells (3, 42)—artifacts due to improper fixation. Although certain other manifestations of inadequate fixation, such as broken cell membranes, swollen mitochondria, and clumped nucleoplasm, are not present in this material, isolated fixation artifacts can occur; the possibility that shrinkage and swelling create these two cell types cannot therefore be dismissed entirely. Nevertheless, this explanation could not by itself account for the fact that in filamented cells, where there is a reduction of some organelles, the concentration of neurofilaments, instead of being correspondingly low, is vastly increased as compared with that in the granular neurons. Furthermore, the almost invariable presence of compact myelin around filamented cells would also not be explained in terms of pure swelling or shrinkage. For these reasons artifact does not seem to be a satisfactory explanation for the existence of the two cell types.

Another possibility, which was considered in some detail in connection with the goldfish acoustic ganglion (38), is that neurons with a reduced concentration of ribosomes may have limited access to nutrient materials owing to their enclosure in a thick compact myelin sheath which could act as a barrier to the passage of materials into them. The paucity of RNP particles and the generally empty appearance of their cytoplasm could then be interpreted as evidence of malnutrition. In the goldfish, cells of this type are surrounded by compact myelin sheaths having about fifty to ninety lamellae. In the rat, however, this is not the case. All the neurons in the ganglion are surrounded by uniformly thin myelin sheaths (about ten lamellae). The two cell types occur randomly throughout the ganglion and there appears to be no difference in their proximity to capillaries. Thus, reduction of RNP concentration in neuronal cytoplasm is probably not simply a reflection of poor nutrition due to the presence of a thick wall around these cells.

Another possible explanation for the occurrence of two neuronal types is suggested by a group of experiments on the effects of physiological activity on the composition of neuronal cytoplasm (19). Determinations of cytoplasmic protein and RNA indicated that the concentrations of these substances change with activity although the direction of change is not always the same. In one series of experiments (15) on the cochlear ganglion of the guinea pig, both protein and RNA concentrations fell significantly following a strong aural stimulus to the living animal. The reduction persisted for about two weeks. Although the stimulus used in these experiments was outside the usual physiological range, smaller-scale changes of the same type could occur in response to normal stimuli. Similarly Brattgård (1) reported that retinal ganglion

cells of newborn rabbits did not develop the usual concentrations of cytoplasmic protein and RNA unless the retinas were exposed to stimulation by light. Thus the observed morphological differences between normal cochlear ganglion cells reported here might be a reflection of different levels of physiological activity in the two groups of cells.

In guinea pigs, there apparently are two populations of fibers in the cochlear nerve (46), which have been termed "high threshold" and "low threshold." A tone pip gave rise to only one or two impulses in the former group, while fibers of the latter variety responded with four to six impulses. It was suggested that the high threshold group may innervate inner hair cells while the low threshold fibers may arise from outer hair cells.

The structural grouping of acoustic ganglion cells into two populations may accordingly reflect either differences in the average level of physiological activity in the two cell types or segregation of their peripheral or central terminations.

I am greatly indebted to Dr. S. L. Palay for providing the specimens used in this study, for his interest and encouragement, and for his critical appraisal of the work. I also wish to thank Dr. Clifford Patlak of the Section on Theoretical Statistics and Mathematics, National Institute of Mental Health, for valuable discussions concerning the electrophysiological interpretations.

Received for publication, July 17, 1961.

REFERENCES

1. BRATTGÅRD, S., The importance of adequate stimulation for the chemical composition of retinal ganglion cells during early post-natal development, *Acta Radiol.*, 1952, Suppl. 96.
2. BRIGHTMAN, M., unpublished observations.
3. CAMMERMEYER, J., The post-mortem origin and mechanism of neuronal hyperchromatosis and nuclear pyknosis, *Exp. Neurol.*, 1960, **2**, 379.
4. CHOI, J. K., Light and electron microscopy of the toad urinary bladder, *Anat. Rec.*, 1961, **139**, 214.
5. DE ROBERTIS, E., GERSCHENFELD, H. M., and WALD, F., Cellular mechanism of myelination in the central nervous system, *J. Biophysic. and Biochem. Cytol.*, 1958, **4**, 651.
6. ENGSTRÖM, H., On the double innervation of the sensory epithelia of the inner ear, *Acta Oto-Laryngol.*, 1958, **49**, 109.
7. FERNÁNDEZ-MORÁN, H., and FINEAN, J. B., Electron microscope and low-angle x-ray diffraction studies of the nerve myelin sheath, *J. Biophysic. and Biochem. Cytol.*, 1957, **3**, 725.
8. FRANKENHAEUSER, B., and HODGKIN, A. L., The after-effects of impulses in the giant nerve fibres of *Loligo*, *J. Physiol.*, 1956, **131**, 341.
9. GASSER, H. S., Properties of dorsal root unmedullated fibers on the two sides of the ganglion, *J. Gen. Physiol.*, 1955, **38**, 709.
10. GAVIN, M. A., and LLOYD, B. J., JR., Knives of high silica content glass for thin-sectioning, *J. Biophysic. and Biochem. Cytol.*, 1959, **5**, 507.
11. GEREN, B. B., The formation from the Schwann cell surface of myelin in the peripheral nerves of chick embryos, *Exp. Cell Research*, 1954, **7**, 558.
12. GEREN, B. B., and SCHMITT, F. O., The structure of the Schwann cell and its relation to the axon in certain invertebrate nerve fibers, *Proc. Nat. Acad. Sc.*, 1954, **40**, 863.
13. GRAY, E. G., Axo-somatic and axo-dendritic synapses of the cerebral cortex, *J. Anat.*, 1959, **93**, 420.
14. HAMA, K., Some observations on the fine structure of the giant nerve fibers of the earthworm, *Eisenia foetida*, *J. Biophysic. and Biochem. Cytol.*, 1959, **6**, 61.
15. HAMBERGER, C., and HYDÉN, H., Cytochemical changes in the cochlear ganglion caused by acoustic stimulation and trauma, *Acta Oto-Laryngol.*, 1945, Suppl. 61.
16. HESS, A., The fine structure and morphological organization of the peripheral nerve-fibres and trunks of the cockroach (*Periplaneta americana*), *Quart. J. Micr. Sc.*, 1958, **99**, 333.
17. HODGKIN, A. L., The ionic basis of electrical activity in nerve and muscle, *Biol. Revs.*, 1951, **26**, 339.
18. HODLER, J., STÄMPFLI, R., and TASAKI, I., Role of potential wave spreading along myelinated nerve fiber in excitation and conduction, *Am. J. Physiol.*, 1952, **170**, 375.
19. HYDÉN, H., The neuron, *in* The Cell, Biochemistry, Physiology, Morphology, (J. Brachet and A. E. Mirsky, editors), New York, Academic Press, Inc., 1960, **4**, 215.
20. KAPLAN, L., Nervenfärbungen. (Neurokeratin, Markscheide, Achsenzylinder.) Ein Beitrag zur Kenntnis des Nervensystems, *Arch. Psychiat.*, 1902, **35**, 825.
21. KOLMER, W., Gehörorgan, *in* Handbuch der mikroskopischen Anatomie des Menschen,

(W. von Möllendorff, editor), Berlin, Julius Springer, 1927, **3**, part 1, 250.

22. LUFT, J. H., Improvements in epoxy resin embedding methods, *J. Biophysic. and Biochem. Cytol.*, 1961, **9**, 409.
23. LUSE, S. A., The fine structure of the morphogenesis of myelin, *in* The Biology of Myelin, (S. R. Korey, editor), New York, Paul B. Hoeber, Inc., 1959, 59.
24. MÜNZER, F. T., Über markhaltige Ganglienzellen, *Z. mikr.-anat. Forsch.*, 1931, **24**, 286.
25. NAUMANN, R. A., and LUSE, S. A., The ultrastructure of myelinated cell bodies of the vestibular ganglion, *Am. J. Anat.*, in press.
26. PALADE, G. E., The fine structure of mitochondria, *Anat. Rec.*, 1952, **114**, 427.
27. PALAY, S. L., MCGEE-RUSSELL, S. M., GORDON, S., and GRILLO, M. A., Fixation of neural tissues for electron microscopy by perfusion with solutions of osmium tetroxide, *J. Cell Biol.*, 1962, **12**, 385.
28. PAPPAS, G. D., Studies on the ciliary epithelium and the zonule. I. Electron microscope observations on changes induced by alteration of normal aqueous humor formation in the rabbit, *Am. J. Ophth.*, 1958, **46**, 299.
29. POTANOS, J. N., WOLF, A., and COWEN, D., Cytochemical localization of oxidative enzymes in human nerve cells and neuroglia, *J. Neuropath. and Exp. Neurol.*, 1959, **18**, 627.
30. RHODIN, J. Correlation of ultrastructural organization and function in normal and experimentally changed proximal convoluted tubule cells in the mouse kidney, Stockholm, Dept. of Anatomy, Karolinska Institutet, 1954.
31. ROBERTSON, J. D., The ultrastructure of adult peripheral myelinated fibers in relationship to myelinogenesis, *J. Biophysic. and Biochem. Cytol.*, 1955, **1**, 271.
32. ROBERTSON, J. D., New observations on the ultrastructure of the membranes of frog peripheral nerve fibers, *J. Biophysic. and Biochem. Cytol.*, 1957, **3**, 1043.
33. ROBERTSON, J. D., The ultrastructure of Schmidt-Lantermann clefts and related shearing defects of the myelin sheath, *J. Biophysic. and Biochem. Cytol.*, 1958, **4**, 39.
34. ROBERTSON, J. D., Structural alterations in nerve fibers produced by hypotonic and hypertonic solutions, *J. Biophysic. and Biochem. Cytol.*, 1958, **4**, 349.
35. ROBERTSON, J. D., The ultrastructure of cell membranes and their derivatives, *Biochem. Soc. Symp.*, 1959, **16**, 3.
36. ROBERTSON, J. D., Preliminary observations on the ultrastructure of nodes of Ranvier, *Z. Zellforsch. u. mikr. Anat.*, 1959, **50**, 553.
37. ROSENBLUTH, J., and PALAY, S. L., Electron microscopic observations on the interface between neurons and capsular cells in dorsal root ganglia of the rat, *Anat. Rec.*, 1960, **136**, 268.
38. ROSENBLUTH, J., and PALAY, S. L., The fine structure of nerve cell bodies and their myelin sheaths in the eighth nerve ganglion of the goldfish, *J. Biophysic. and Biochem. Cytol.*, 1961, **9**, 853.
39. ROSS, L. L., BORNSTEIN, M., and LEHRER, G., Electron microscopic observations on myelin sheath formation in tissue cultures of developing rat cerebellum, *Anat. Rec.*, 1960, **136**, 268.
40. SCHARF, J. H., Untersuchungen an markhaltigen Ganglienzellen in der Wirbeltierreihe und beim Menschen, *Anat. Anz.*, 1950, **97**, Suppl., 207.
41. SCHARF, J. H., Sensible Ganglien, *in* Handbuch der mikroskopischen Anatomie des Menschen, (W. von Möllendorff and W. Bargmann, editors), Berlin, Springer-Verlag, 1958, **4**, part 3, 280.
42. SCHARRER, E., On dark and light cells in the brain and in the liver, *Anat. Rec.*, 1938, **72**, 53.
43. SCHMITT, F. O., Ultrastructure of nerve myelin and its bearing on fundamental concepts of the structure and function of nerve fibers, *in* The Biology of Myelin, (S. R. Korey, editor), New York, Paul B. Hoeber, Inc., 1959, 1.
44. SCHMITT, F. O., BEAR, R. S., and CLARK, G. L., X-ray diffraction studies on nerve, *Radiology*, 1935, **25**, 131.
45. STENGER, R. J., and SPIRO, D., The ultrastructure of mammalian cardiac muscle, *J. Biophysic. and Biochem. Cytol.*, 1961, **9**, 325.
46. TASAKI, I., Nerve impulses in individual auditory nerve fibers of guinea pig, *J. Neurophysiol.*, 1954, **17**, 97.
47. TASAKI, I., New measurements of the capacity and the resistance of the myelin sheath and the nodal membrane of the isolated frog nerve fiber, *Am. J. Physiol.*, 1955, **181**, 639.
48. UZMAN, B. G., and NOGUEIRA-GRAF, G., Electron microscope studies of the formation of nodes of Ranvier in mouse sciatic nerves, *J. Biophysic. and Biochem. Cytol.*, 1957, **3**, 589.
49. VILLEGAS, G. M., and VILLEGAS, R., The ultrastructure of the giant nerve fibre of the squid: axon-Schwann cell relationship, *J. Ultrastruct. Research*, 1960, **3**, 362.
50. VILLEGAS, R., and VILLEGAS, G. M., Characterization of the membranes in the giant nerve fiber of the squid, *J. Gen. Physiol.*, 1960, **43**, 73.
51. WATSON, M., Staining of tissue sections for electron microscopy with heavy metals, *J. Biophysic. and Biochem. Cytol.*, 1958, **4**, 475.
52. WEBSTER, H. DE F., and SPIRO, D., Phase and electron microscopic studies of experimental

demyelination, *J. Neuropath. and Exp. Neurol.*, 1960, **19**, 42.

53. Weiss, J. M., Mitochondrial changes induced by potassium and sodium in the duodenal absorptive cell as studied with the electron microscope, *J. Exp. Med.*, 1955, **102**, 783.

54. Wolf, A., Cowen, D., and Antopol, W., Reduction of neotetrazolium in the satellite cells of the spinal and sympathetic ganglia, *J. Neuropath. and Exp. Neurol.*, 1956, **15**, 384.

55. Wolff, D., The ganglion spirale cochleae, *Am. J. Anat.*, 1936, **60**, 55.